

FAIR sharing of Chromatin Tracing datasets using the newly developed 4DN FISH Omics Format

Authors

Rahi Navelkar ^{a#}, Andrea Cosolo ^{a#}, Bogdan Bintu ^b, Yubao Cheng ^c, Vincent Gardeux ^d, Silvia Gutnik ^e, Taihei Fujimori ^f, Antonina Hafner ^g, Atishay Jay ^h, Bojing Blair Jia ⁱ, Adam Paul Jussila ^j, Gerard Llimos ^d, Antonios Lioutas ^k, Nuno M. C. Martins ^k, William J Moore ^l, Yodai Takei ^m, Frances Wong ^l, Kaifu Yang ⁿ, Huaiying Zhang ^o, Quan Zhu ⁿ, Magda Bienko ^p, Lacramioara Bintu ^f, Long Cai ^m, Bart Deplancke ^d, Marcelo Nollmann ^q, Susan E Mango ^e, Bing Ren ⁿ, Peter J Park ^a, Ahilya N Sawh ^r, Andrew Schroeder ^a, Jason R. Swedlow ^l, Golnaz Vahedi ^h, Chao-Ting Wu ^k, Sarah Aufmkolk ^{k#}, Alistair N. Boettiger ^{g#}, Irene Farabella ^{s#}, Caterina Strambio-De-Castillia [#], Siyuan Wang ^{c#}
[#], Contributed equally to this work.

Affiliations

a - Department of Biomedical Informatics, Harvard Medical School, Boston, MA 02115, USA

b - Shu Chien-Gene Lay, Department of Bioengineering, University of California, San Diego, La Jolla, CA, USA

c - Department of Genetics, Yale University, New Haven, CT 06510, USA

d - Laboratory of Systems Biology and Genetics, Institute of Bioengineering, School of Life Sciences, Ecole Polytechnique Fédérale de Lausanne (EPFL), Lausanne, Switzerland

e - Biozentrum, University of Basel, Basel, BS, CH

f - Department of Bioengineering, Stanford University, Stanford, CA 94305, USA

g - Department of Developmental Biology, Stanford University, Stanford, CA 94305, USA

h - Department of Bioengineering, University of Pennsylvania

i - Bioinformatics and Systems Biology Graduate Program, University of California San Diego, La Jolla, CA, USA; Medical Scientist Training Program, University of California San Diego, La Jolla, CA

j - Bioinformatics and Systems Biology Graduate Program, University of California San Diego, La Jolla, CA, USA

k - Department of Genetics, Harvard Medical School, Boston, MA 02115, USA

l - Divisions of Molecular Cell and Developmental Biology and Computational Biology, University of Dundee, Dundee, UK

m - Division of Biology and Biological Engineering, California Institute of Technology, Pasadena, CA, USA

n - Center for Epigenomics, Department of Cellular and Molecular Medicine, School of Medicine, University of California, San Diego, La Jolla, CA, USA

o - Carnegie Mellon University, Department of Biological Sciences, Pittsburgh, PA, 15213, USA

p - Human Technopole, Milan, Italy; Department of Microbiology, Tumor and Cell Biology, Karolinska Institutet, SciLifeLab, Stockholm, Sweden

q - Center of Structural Biology, Univ Montpellier, CNRS, INSERM, Montpellier, France

r - Department of Biochemistry, University of Toronto, Toronto, Ontario, Canada

s - Integrative Nuclear Architecture Laboratory, Center for Human Technologies, Istituto Italiano di Tecnologia, Genova, Italy.

t - Program in Molecular Medicine, UMass Chan Medical School, Worcester, MA 01605, USA

Abstract

In recent years, multiplexed Fluorescence In Situ Hybridization (FISH) or FISH-omics methods have rapidly expanded, enabling the quantification of chromatin organization in single cells, often in conjunction with measurements of RNA and protein. These approaches have deepened our understanding of how 3D chromosome architecture relates to transcriptional activity and cell states in health and disease. Despite these advances, results from Chromatin Tracing FISH-omics experiments remain challenging to share, reuse, and analyze due to the absence of standardized data exchange specifications. Building on the release of microscopy metadata standards, we introduce the FISH Omics Format-Chromatin Tracing (FOF-CT), a community-developed standard for processed results from diverse imaging modalities. We describe the FOF-CT file format and present a curated collection of datasets deposited in the 4D Nucleome Data Portal and the OME Image Data Resource (IDR). We also highlight their potential for reuse, integration, and modeling by outlining example analysis pipelines and illustrating biological insights enabled by standardized, FAIR-compliant Chromatin Tracing datasets. While this manuscript focuses on the representation of ball-and-stick Chromatin Tracing, the format is designed to be extensible to volumetric Chromatin Tracing.

Introduction

The 4D Nucleome (4DN) project ¹⁻³ aims to understand the three-dimensional organization and complex structure of chromatin in four dimensions by incorporating elements of time and space. In this context, a significant focus is on mapping the dynamics of chromosome and nuclear organization, as well as the variations observed between single cells. To this aim, in addition to sequencing-based techniques such as high-throughput Chromosome Conformation Capture (Hi-C), a variety of microscopy-based Fluorescence In-Situ Hybridization (FISH) techniques are employed.

Classical DNA FISH utilizes fluorescently labelled DNA probes to visually identify specific parts of the genome and capture images of these labeled segments within individual cells, as reviewed by ⁴⁻⁹. Advances in hybridization protocols, microfluidics systems, and the construction of large arrays of barcoded targeting oligonucleotides (including Oligopaints) ¹⁰⁻¹⁴ have expanded the capability of DNA FISH to image multiple DNA segments to potentially cover the entire genome, as reviewed by ^{5,15-21}. These methods are interchangeably referred to as **DNA Multiplexed FISH** or **FISH omics** [reviewed in ²], highlighting their common objective of mapping the positions of numerous specific DNA segments, often in conjunction with localizing other cellular components like RNA and proteins ^{19,22-32}.

A variety of DNA FISH Omics protocols have been developed in recent years, where the 3D configuration of chromatin is reconstructed by connecting the location of targeted segments captured in successive rounds in a genomic mapping process known as “Chromatin Tracing”, as demonstrated by ²⁶. Chromatin Tracing techniques can be categorized into two main types (see Figure 2 in Dekker et al.)²: **ball-and-stick** ^{22-24,26-58} or **volumetric** ^{46,59-63}. The distinction between these methods lies in how they visualize the genomic Targeted Segment (Supplemental Table I - Glossary). The distinctive feature of ball-and-stick Chromatin Tracing methods is that the fluorescent spot observed during each hybridization cycle corresponds to the entire targeted genomic segment, typically ranging from 2 to 100 kilobases. On the other hand, volumetric Chromatin Tracing techniques depict the segment as a cloud of single-molecule localizations, often rendered as a volume, wherein each localization represents just one of the multiple fluorophore molecules used to target the segment.

The inherently 3D nature of Chromatin Tracing data enables multi-faceted characterization of chromatin folding conformation through a range of quantitative metrics, thereby revealing novel biological and biophysical insights ⁶⁴. At the population level, contact frequency or spatial distance matrices derived from Chromatin Tracing closely recapitulate widely used Hi-C contact maps, capturing both quantitative values and qualitative patterns, including key features such as A/B compartments ⁶⁵, topologically associating domains (TADs), and promoter–enhancer interactions ^{22,26,30,36-39,42-44,46,47,66,67}. At the single-cell and single-trace level, spatial distance matrices derived from Chromatin Tracing experiments unveil structural variability across all genomic scales, for example, demonstrating variability in physically segregated A/B compartments ^{23,24,26,31,41,44,47,60}, and highly variable TAD-like structures ^{22,24,46,47} (also referred to as single-cell domains). Notably, such domain variability has been observed even in the absence of loop extrusion and major epigenetic modifications ⁶⁸, suggesting that additional mechanisms contribute to chromatin organization beyond canonical extrusion-based models ^{44,46,50,69}. While plaid-patterned contact enrichment, indicative of separation into A/B compartments, is observed at the population level and appears to be conserved across diverse cell types, the single-cell nature of Chromatin Tracing reveals a more distinct behavior. For example, in mature and slowly dividing cells, individual chromosomes in single cells often partition into physically separated A/B compartments ^{23,24,60,70}. In contrast, it has been shown that in embryonic stem cells, the compartments exhibit a statistical enrichment of contacts, with individual chromosomes in single cells rarely fully segregating all their A and B regions into two physically distinct domains ^{27,28,33}. Chromatin Tracing data also enable the analysis of multi-way contacts ^{32,38,40,44,46,52,67,71}, facilitating the discovery of functional cross-TAD and long-range regulatory interactions mediated by multiple loops ^{38,44,67,59}. Chromatin Tracing derived spatial distance matrices also enable quantitative assessment of chromosome compaction by comparing whether distances systematically change across conditions ^{26,29,31,36-38,41,46,55}. Alternatively, compaction can also be estimated from radii of gyration in contiguous ball-and-stick or volumetric chromatin traces ^{23,26,29,31,36,37,41,46,47,55,57,60,61,63,72}. Chromatin Tracing provides insights into genome-scale spatial organization at a macro scale by quantifying the radial distribution of each locus within the nuclear space in a genome-wide Chromatin Tracing experiment ^{27,28,55} and revealing the proximity between genomic loci and nuclear landmarks (such as nuclear lamina, nucleoli, and nuclear speckles)⁷³ or epigenetic compartments ^{23,24,27,41}. As a result, FISH-

Omics has transformed genome organization studies by enabling single-cell visualization and quantification of chromatin architecture across scales, revealing the importance of structural variability^{22–24,26–31,33–44,46,59–63}.

While this rapid technological progress has driven significant advances, it has also led to a lack of standardization. As individual labs optimized their own pipelines for data acquisition, storage, and analysis, a diversity of bespoke formats and workflows emerged, resulting in a fragmented data-format landscape. The resulting proliferation of incompatible data structures makes cross-study comparisons arduous. However, re-analysis of single-cell Chromatin Tracing datasets has resulted in several novel insights into genome organization and function. For instance, Bohrer and Lason⁷⁴ showed that gene co-expression is driven by physical proximity rather than genomic distance. Rajpurkar et al.³⁰ utilized nascent RNA-labeled Chromatin Tracing data from the *Drosophila* Bithorax Complex to link chromatin architecture to transcriptional state, revealing that redundant structural layers and rare long-range contacts contribute to transcriptional silencing. Goundaroulis et al.⁷⁵ examined single-cell traces from a 2-Mb Targeted Region (Supplemental Table I - Glossary) on human chromosome 21⁴⁶ and demonstrated that interphase chromatin is predominantly unknotted at the megabase scale, with most observed knots attributable to localization errors in densely packed regions, highlighting the need for rigorous quality control. Patel et al. used Chromatin Tracing data from human and mouse cells^{27,28,46,76} to develop a method for detecting chromatin domain-like structures and boundaries in single-chromosome pairwise distance matrices, even with substantial missing data. Liefsoens et al.⁷⁷ introduced A-Plot, a spectral approach that, in conjunction with neural networks, detects nested and complex chromatin loop structures at both the single-cell and population levels using datasets from Bintu et al.⁴⁶ and Takei et al.²⁷. Several studies developing models for reconstructing the 3D genome have leveraged Chromatin Tracing for both model generation and validation (e.g., Refs. ^{60,78–84}). Recent work by Remini et al.^{85,86} showed that chromatin exhibits two distinct scaling regimes across 5 kb to 2 Mb, both in mouse and in human, corresponding to alternating phases that undergo microphase separation. This observation provides a valuable framework to inform and refine polymer physics models of chromatin organization. Additionally, the increasing availability of public single-cell CT datasets further supports the development⁸² and validation^{87,88} of accurate, multiscale, data-driven 3D chromatin models.

Such efforts have advanced our understanding of genome organization at the single-cell level. However, their broader impact is often limited by inconsistencies in data formats that hinder data portability and reuse. To support reproducibility and facilitate meaningful cross-study comparisons, the adoption of standardized Microscopy Metadata specifications^{89,90}, data formats and robust quality assessment frameworks is essential. Addressing this critical bottleneck, the 4DN Consortium has taken the lead in developing the FISH-Omics Format for Chromatin Tracing (FOF-CT), a standardized framework designed to unify the representation of DNA FISH data across platforms and studies. The rationale for creating the FOF-CT is to enable the large-scale integration of datasets across different model systems, experimental conditions, and analytical modalities; streamline the development of computational tools, including machine learning applications for spatial genomics; and enhance reproducibility by ensuring compliance with FAIR (Findable, Accessible, Interoperable, Reusable) principles. This manuscript describes the development of 4DN FOF-CT, a standardized data format designed to capture and share results from DNA FISH Omics imaging experiments. This format is immediately compatible with all ball-and-stick Chromatin Tracing techniques described above and is designed to be easy-to-extend to support volumetric methods in the future.

An exchange format for the results of FISH Omics Chromatin Tracing experiments

In **ball-and-stick Chromatin Tracing** experiments, polymer tracing algorithms are used to connect the localization of individual DNA-FISH bright Spots (Supplemental Table I - Glossary) and reconstruct the three-dimensional (3D) path of chromatin fibers. While a full description of the proposed FOF-CT specifications can be found on ReadTheDocs⁹¹, a short summary is provided here.

FOF-CT is organized in a modular fashion, ensuring the standardization of essential Chromatin Tracing data arising from multiple individual techniques, while providing the flexibility necessary to capture additional data that may be required only in specific experimental designs (Figures 1 and 2). Thus, while all FOF-CT-compliant datasets must include at least one TXT, CSV, or TSV file, they might contain up to twelve files, each containing one of the individual interlinked

prescribed tables (Figures 1 and 2). Specifically, the core of the format consists of the **mandatory DNA-Spot/Trace** core table (i.e., *Table 1*) that defines Chromatin Traces as ordered lists of individual DNA-FISH bright Spots. Specifically, this table reports the XYZ coordinates with respect to the microscopy detection system of individually detected DNA bright Spots, the BED⁹² specified genomic location of their target Segment (i.e., Chrom, Chrom_Start, Chrom_End), their Trace assignment as well as their Cellular, Extracellular and Sub-Cellular Region of Interest (ROI) allocation, if appropriate. Additional highly recommended tables, which are linked with the Core table by way of deposition-wide or (ideally) globally unique identifiers (UIDs; Figure 2), support the integration of core Chromatin Tracing results with:

- 1) The list of individual localizations that are used to identify individual bright Spots with combinatorial barcoding (i.e., *Table 2 - Spot Demultiplexing*).
- 2) Global **Trace**-level experimental results, such as the expression level of nascent RNA transcripts associated with a given Trace or overall localization of the Trace with respect to cellular or nuclear landmarks (i.e., *Table 3 - Trace Data table*).
- 3) The results of **Multiplexed RNA-FISH** experiments conducted in parallel with the main Chromatin Tracing experiment (i.e., *Table 4 - RNA Spot Data*)²⁴.
- 4) Supplemental Spot properties such as **Quality metrics** (i.e., *Tables 5 - Spot Quality* and *6 - RNA_Spot Quality*) and **Physical coordinates** (i.e., *Tables 7 - Spot Biological Data* and *8 RNA_Spot Biological Data*) mapping the position of bright Spots with respect to landmarks defining the architectural organization of the cellular and nuclear space^{27,28}.
- 5) Experimental results that are better captured at the global level of **Cell** (i.e., *Table 9 - Cell Data*; e.g., boundaries and volume), **Extracellular Region of Interest (ROI)** (i.e., *Table 10 - Extra-Cell ROI Data table*; e.g., Tissue), and **Sub-cellular ROI** (i.e., *Table 11 - Sub-Cell ROI Data*; e.g., Nuclear feature or Nucleolus)^{18,22-28}.
- 6) The boundaries of individual Cells and other Extracellular and Sub-cellular ROIs that were identified as part of the experiment (i.e., *Table 12 - Cell/ROI Mapping*).

In keeping with the modular nature of FOF-CT, all tables are organized in the same general manner and must include two mandatory components: 1) a **header section containing metadata fields**, represented as key-value pairs providing essential information about the experiment and table content and each occupying an individual header line; and 2) a **column section reporting the actual experimental results** in a tabular format. The following rules apply to all table items: 1) Metadata field (i.e., keys) and Column names must use the underscore as a word separator (e.g., *RNA_A_intensity*). 2) Metadata fields and Columns can be required, conditionally required, or optional, where conditionally required items are required only when certain conditions are met (e.g., *##intensity_unit*= is required any time an intensity metric is reported). In the **header section**, each line is denoted by the hashtag symbol (i.e., #) and must contain an individual metadata field. Specifically, three different types of header metadata fields are possible:

- 1) **Human-readable metadata.** These lines must be prefixed with “#” and use the **#key: value** format (e.g., *#lab_name*: name of the lab where the experiment was performed).
- 2) **Mandatory machine-readable metadata.** These lines must be prefixed with “##” and follow the **##key=value** format (e.g., *##FOF-CT_version=v0.1*).
- 3) **User-defined column description.** These lines provide the name and description of optional, user-defined data columns. Descriptions must be understandable and sufficient to ensure the interpretation and reproducibility of the results. These lines must be prefixed with “#^” and follow the **#^key: value** format (e.g., *#^optional_column_1*: optional column 1 description).

In the **column section**, the first column must always be a relevant UID, such as *Spot_ID*, *Trace_ID*, *Cell_ID*, etc. All other columns must either be mandatory, depending on the table type, or provided at the user’s discretion and must be mandatorily defined in the file header as described above. Unless specified, the column and row order is at the user’s discretion. If an optional column contains no data (i.e., it is not used), it should be omitted.

To promote interoperability across different genomic modifications, FOF-CT provides instructions for reporting the location of DNA Spots and Traces in case the genome under study contains insertions or deletions⁹¹. In summary, users are

required to provide the following information to relate the location of targeted genomic Segments with respect to the modified genome: 1) a description of the nature and location of the genomic modification; 2) a supplemental Variant Call Format (VCF)⁹³ file to report the nature and location of the genome modification; 3) the name of the inserted or deleted DNA fragment; and 4) the Start and End coordinates of the target chromosome Segment with respect to the insertion or deletion.

4D Nucleome Data Portal published FOF-CT datasets

The 4DN data portal⁹⁴, part of the 4DN Data Coordination and Integration Center (DCIC), is a repository for datasets generated within and outside the 4DN project. Currently, the portal hosts over 2679 publicly available datasets generated using ~47 different sequencing assays and ~7 imaging techniques from at least 108 publications. Recognized by unique 4DN identifiers, these datasets can be easily browsed, visualized, and freely downloaded from the 4DN data portal (<https://data.4dnucleome.org>). The metadata from different studies, often in collaboration with the authors, is expertly curated and standardized according to the established 4DN data schema and model (<https://data.4dnucleome.org/help/user-guide/data-model>).

Figure 3 and Supplemental Table II supply a summary and detailed description, respectively, of 212 public imaging datasets (209 available on the 4DN Data Portal and 3 available on Image Data Resource - IDR; see below) associated with 28 publications (27 available on the 4DN Data Portal and 1 available on IDR)^{22–24,26–28,31,32,36,38,39,41,43–58} that provide data in FOF-CT format and were deposited by laboratories that either belonged to the 4DN consortium (Figure 3, *light blue*) or were External to it (Figure 3, *dark blue*). In Supplemental Table II, each row refers to a group of datasets, which were generated as part of a single publication. Importantly, the table comprises datasets from both 4DN-affiliated laboratories and the broader community, demonstrating the widespread adoption of the format beyond 4DN. The table comprises datasets generated by targeting various cells or tissues from humans, mice, *C. elegans*, and fruit flies using Chromatin Tracing techniques, including multi-omic ORCA, Hi-M, MINA, MERFISH, and seqFISH. The imaging results, regardless of the techniques used, are standardized by adhering to the FOF-CT format (<https://data.4dnucleome.org/resources/data-collections/chromatin-tracing-datasets>). The processed files, along with the curated metadata, follow the usual data submission and quality control process and are made available on the 4DN portal (<https://data.4dnucleome.org/microscopy-data-overview>). Importantly this includes a detailed description of the hardware configuration of each microscope that was used for image acquisition, which is provided in compliance with the Light Microscopy (LiMi) - Model of Metadata specifications (previously known as 4DN-BINA-OME-QUAREP - NBO-Q)⁸⁹. A list of the Micro-Meta App^{90,95} produced Microscope-Hardware JSON files associated with each publication is available in Supplemental Table III.

Imaging data submission of this type requires collaboration between data generators, subject matter experts, and data curators and has led to significant advancements in developing data models, metadata schemas, and community-wide accepted data exchange standards for imaging data. Recent packages for the analysis and post-processing of multiplexed DNA-FISH data took a step in this direction by making FOF-CT one of their output and input formats (e.g. pyHiM, traceratops or the Chromatin IMaging Analysis (CIMA) tool^{96,97}. As a result, researchers can leverage quality-controlled, standardized, and AI-ready datasets to effortlessly share and transfer data, perform large-scale, complex downstream analysis, and generate visualization tools in a manner previously unattainable. Further evidence of widespread adoption of FOF-CT is provided by the adoption of the format by third-party repositories such as IDR.

FOF-CT adoption by the OME Public Image Data Resource (IDR)

IDR is a public image repository with a focus on metadata to provide added value to imaging data for the scientific community⁹⁸. This added value comes from the inclusion of experimental metadata, biomolecular annotations, and analysis results that are linked to the image data via curation. Experimental metadata, such as the specimen, sample preparation, and details of chemical or genetic perturbations, can be valuable to many users, as it allows them to understand and track specific details of the work. Additionally, metadata on imaging modalities, as well as staining and/or contrast methods where applicable, are essential for enabling the interpretation and analysis of any dataset. The curation of data in IDR can identify

and correct errors, omissions, and inconsistencies in image data and metadata, which is an important step towards adhering to the FAIR principles. Additionally, capturing and maintaining accurate metadata is essential to ensuring that data is reliable, reusable, and accessible to the scientific community. Furthermore, standardized metadata is required to enable users to better understand specialized terms and to allow meaningful comparisons with other datasets. This can be achieved by utilizing controlled vocabularies, such as common terms from public ontologies. IDR utilizes standardized ontologies to link datasets and facilitate establishing data connections within and between databases.

IDR has to date received two submissions that include multiplexed FISH omics data, Payne et al.³⁵, and Mota et al.⁴⁸, highlighting the need for consistent annotation to facilitate the reuse of this data alongside other FISH omics studies. IDR collaborated with the 4DN FISH omics team to incorporate the FOF-CT standardized terms into the analysis results tables, which correspond to the Core FOF-CT table (see the example table at https://idr.openmicroscopy.org/webclient/omero_table/43412838/). These tables are assigned a unique namespace in IDR, allowing all such tables to be retrieved via the IDR's API. Tabular data in IDR can be queried by values in the rows, supporting the search for Spots according to Chromosome position, image coordinates, and other attributes. The Spot_ID refers to a Shape identifier in IDR that can be used to view the spot in a multi-dimensional image viewer (see example at <https://idr.openmicroscopy.org/iviewer/?shape=7219651>). The IDR team encourages the submission of additional datasets annotated with FOF-CT terms to enhance the community's access to publicly available FISH omics data.

The widespread adoption of FOF-CT facilitates data sharing and empowers downstream visualization and analysis of 4DN imaging data

Adopting the FISH-Omics Format for Chromatin Tracing (FOF-CT) establishes a standardized framework that ensures the integration and re-analysis of Chromatin Tracing datasets from diverse protocols, sample types, and data modalities. By enforcing structured metadata and consistent coordinate representation, FOF-CT enhances data reuse and facilitates meaningful comparisons across studies and laboratories, thereby supporting cumulative efforts to build larger and more integrative datasets. Notably, the ongoing deposition of FOF-CT-compliant datasets, with over 200 datasets from 28 publications within a four-year period, reflects growing community engagement.

The development of structural inference and detection methods is a practical example of the value of standardized, shareable Chromatin Tracing data. For instance, Jia et al.⁴⁹ re-analyzed multiple ball-and-stick Chromatin Tracing experiments^{27,28} to introduce a spatial genome aligner for chromatin trace reconstruction that accounts for copy number variations and aneuploidy. Building on early work in chromatin trace reconstruction⁹⁹, this tool opens new avenues for exploring chromatin architecture in genetically complex samples. Similarly, Lee et al. developed SnapFISH (Single-Nucleus Analysis Pipeline for multiplexed DNA FISH)¹⁰⁰, a computational approach for detecting chromatin loops across Chromatin Tracing experiments at different genomic resolutions, considering pairwise chromatin interaction data. Their method was validated across multiple datasets^{22,27,28,101}, underscoring the power of standardized data formats to facilitate robust cross-study analyses. More recently, Yu et al. introduced ArcFISH (Accurate and Robust Chromatin analysis from FISH data)¹⁰² a novel computational approach that explicitly models the three-dimensional, xyz-axis-specific measurement errors inherent in Chromatin Tracing in a unified statistical framework to detect multi-level 3D genome features. By treating each spatial axis separately, ArcFISH fully exploits the rich information contained in the raw traces. Extensive benchmarking on diverse FOF-CT-compliant Chromatin Tracing datasets—including mouse and human samples and multiple imaging protocols—demonstrates that ArcFISH consistently surpasses existing pipelines in accuracy, interpretability, and biological relevance.

In addition, the availability of standardized, shareable Chromatin Tracing datasets has enabled the development of imputation strategies to address missing data, an inherent limitation in high-resolution Chromatin Tracing experiments. Due to limited detection efficiency, particularly in protocols with multiple hybridization rounds, most ball-and-stick datasets with sub-30 kb genomic resolution report detection rates below 80%^{22,24,27,29,43,100}. Initial imputation efforts relied on local smoothing strategies, such as averaging pairwise distances across neighboring loci²⁷ or across single cells⁴¹, and coordinate

interpolation from adjacent spots⁴³. While effective in specific contexts, these approaches are limited in their ability to capture global structural features.

Recent advances exploit the growing number of publicly available datasets to improve imputation performance. SnapFISH-IMPUTE¹⁰³ identifies similar chromosomal conformations across cells to reconstruct missing loci while preserving local features and global heterogeneity. In parallel, ImputeHiFi¹⁰⁴ integrates Chromatin Tracing with orthogonal single-cell modalities (Hi-C, RNA-seq, RNA FISH) to inform imputation based on multimodal similarity. Together, these tools exemplify how increased data sharing enables more sophisticated analysis pipelines and deeper insights into 3D genome architecture.

The availability of single-cell Chromatin Tracing datasets has opened new avenues for the development of quantitative, data-driven 3D genome modeling, for instance, to generate⁸² and validate⁸⁸ chromatin folding models at multiple genomic scales. These models help bridge the gap between experimental imaging data and population-level chromatin conformations. As more Chromatin Tracing datasets become available in a harmonized format, they will increasingly support the integration of experimental measurements into predictive and mechanistic 3D genome models.

Efforts to standardize Chromatin Tracing data also enable new tools for interactive visualization. The Nucleome Browser¹⁰⁵, originally developed for IDR data, is being explored for integration with FOF-CT datasets on the 4DN Data Portal. Such tools will enhance interactive exploration of Chromatin Tracing data across studies.

The FOF-CT format has the potential to be a powerful tool for searching, visualizing, analyzing, and re-analyzing Chromatin Tracing data, advancing our ability to investigate the spatial organization of chromosomes and gain a mechanistic understanding of 3D genome function.

Future Directions

The primary objective of the 4DN project is to expedite the dissemination of technological and scientific advances by sharing its developed tools and generated data openly and unhinderedly with the broader community. In genomics, data sharing is already well-established, with sequencing data routinely disseminated using well established standardized file formats^{106,107} including the Browser Extensible Data (BED)⁹², and Variant Call Format (VCF)⁹³. As a prerequisite for peer review, most journals enforce strict policies for raw sequencing data—such as RNA-seq—requiring adherence to standards set by community initiatives¹⁰⁸ including the Encyclopedia of DNA Elements (ENCODE)¹⁰⁹ and others^{108,110}, and their deposition into public repositories like the Gene Expression Omnibus (GEO) or Sequence Read Archive (SRA). This ensures data transparency, reproducibility, and long-term accessibility, and have since become standard expectations in genomics, proteomics and structural biology research^{111,112}. The value of these standardized, open-access resources is well-documented: they foster collaboration, accelerate discovery, and drive the development of novel analytical and visualization tools. A striking example of their impact is the 2024 Nobel Prize in Chemistry¹¹³, which recognized breakthroughs in computational protein design and structural prediction—advancements that relied heavily on large, high-quality, and standardized datasets for training predictive algorithms.

However, no such uniform requirement exists for genomic imaging data. As a result, imaging data is often summarized in figure panels without providing access to the underlying data. Consequently, FISH-based image data are not yet routinely made publicly available upon publication, despite their critical role in elucidating chromatin architecture and its implications for gene regulation, development, and disease. The field is rapidly evolving, with an expanding repertoire of FISH Omics techniques, including LoopTrace^{114–116}, Genome Oligopaint via Local Denaturation (GOLD) FISH¹¹⁷, Nanoscopy-compatible Oligonucleotides with dyes in Variable Arrays (NOVA) probes¹¹⁸, Tn-5FISH¹¹⁹, FRET-FISH¹²⁰, or pooled genetic screening methods such as Perturb-tracing⁵⁷. However, this rapid growth also raises concerns about data fragmentation, underscoring the urgent need for shared, extensible, and interoperable exchange formats to integrate diverse datasets into a unified framework.

To address this challenge, the 4DN Imaging Working Group developed FOF-CT, a standardized format designed to facilitate high-quality FISH Omics data production and FAIR data exchange¹²¹. Its modular architecture ensures adaptability to both established and emerging multiplexed FISH techniques, making it a versatile solution for the field.

Additionally, the modular, table-based design is compatible with the SpatialData format (recently introduced for large-scale spatial omics in biological tissues)¹²², thereby paving the way for future integration of spatial omics across scales. The impact of FOF-CT has been profound: since its introduction, adoption has surged, as evidenced by the exponential increase in FOF-CT-compliant datasets deposited in the 4DN Data Portal and on the IDR (Figure 3; Supplemental Table II). Its utility extends beyond 4DN-affiliated laboratories, with independent research groups and public repositories like the OME IDR integrating the format into their workflows. This widespread acceptance highlights both the unmet need that FOF-CT addresses and its pivotal role in advancing 3D genomics research.

The functional study of how nuclear spatial organization influences health and disease demands that we combine sequencing-based methods (e.g. Hi-C) with imaging techniques (e.g. Chromatin Tracing) across many tissue types, cellular states (e.g., cell-cycle phases, differentiation stages, responses to stress), experimental conditions, and labs. Because this data is so varied and complex, interpreting both sequencing- and imaging-based chromatin spatial organization data requires a direct assessment of how “nuclear topography” affects nuclear function. Consequently, efforts initiated by 4DN are underway to create a standardized nuclear reference coordinate system to embed within the FOF-CT. This common coordinate framework (CCF) would anchor imaged chromosome regions within the nucleus, enabling easier data integration, supporting predictive modeling, and increasing the utility of both Hi-C and Chromating Tracing datasets for computational researchers and the broader scientific community.

The development of FOF-CT represents more than a technical milestone—it signifies a maturation of the DNA FISH omics field. By establishing a common language for Chromatin Tracing data, FOF-CT has eliminated interoperability barriers, fostered collaboration, and accelerated computational innovation. In doing so, it has emerged as the gold standard for multiplexed DNA FISH data, ensuring that the full potential of this transformative technology can be realized.

Acknowledgments

This project could never have been carried out without the leadership, insightful discussions, support, and friendship of all OME consortium members, with particular reference to Josh Moore, Chris Allan, and Jean Marie Burel. We are massively indebted to the RIKEN community for their fantastic work to bring open science into biology. We would like to particularly acknowledge Shuichi Onami for his friendship and support. We thank all members of the 4D Nucleome Imaging Standard Working Group, Data Coordination and Integration Center, and NIH leadership team for the vision and encouragement that allowed us to get this project started. We are particularly grateful to Burak Alver, Ian Fingerman, and John Satterlee. We thank all members of BioImaging North America (in particular Judith Lacoste, Nikki Bialy, Claire M. Brown, Alex Cotten, Kevin Eliceiri, Alison North, Vanessa Ott), German Bioimaging (in particular Stephanie Wiedkamp-Peters), Euro-Bioimaging (in particular Johanna Bischof, Antje Keppler and Yara Reis) and QUAREP-LiMi (in particular Roland Nitschke, Aastha Mathur and all members of the Working Group 7 - Metadata; quarep.org) for invaluable intellectual input, fruitful discussions, advice and moral support. The authors wish to thank all personnel at their home core facilities and their institutions for unwavering support and material help in the absence of which this work could not have been successfully concluded. We are also indebted to the following individuals for their continued and steadfast support: Alicia Birtz, Roger Davis, Kathy Gemme, Jeremy Luban, and Andrea Sjostedt at the University of Massachusetts Medical School.

This work was supported by funding provided to the following authors:

WJM, FW, and JRS - W.J.M., F.W., and J.R.S - OME's work described here was funded by the Wellcome Trust (Ref. 221361/Z/20/Z and 313803/Z/24/Z) and a National Institutes of Health Common Fund 4D Nucleome Program grant UM1HG011593.

HZ - H.Z was supported by NIH (U01CA260851)

QZ - NIDA/PA-20-272 (Shen)

MB - M.B. is supported by the Swedish Research Council (grant. no. 2020-02657), Karolinska Institutet (KI Consolidator Grants 2020), and the European Union (ERC, RADIALIS, GA n. 101088408). Views and opinions expressed are those of the authors only and do not necessarily reflect those of the European Union or the European Research Council Executive Agency. Neither the European Union nor the granting authority can be held responsible for them.

LB - L.B. was supported by NIH U01DK127419

MN - M.N. was supported by ANR grants ANR-23-CE12-0023-01, ANR-24-EXCI-0002, ANR-24-CE12-2240-02 and by ERC grant 724429.

SEM - S.E.M. was supported by SNF 310030_197713 and SNF 320030-227954.

BR - B.R. was supported by UM1 HG011585.

PJP - P.J.P was supported by U01CA200059.

ANS - A.N.S. was supported by the Natural Sciences and Engineering Research Council of Canada (NSERC, RGPIN-2024-04767), the Canadian Institutes of Health Research (CIHR, PJT-197921), a Canada Research Chair in 4D Genomics (CRC, 2023-00193), and a Human Frontier Science Program Research Grant (RGP007/2025).

GV - G.V. was supported by the Burroughs Welcome Fund, the Chan Zuckerberg Initiative Award, W. W. Smith Charitable Trust, the Sloan Foundation, and the NIH grants UC4 DK112217, U01 DK112217, R01 HL145754, R01AI168240, U01 DK127768, U01 DA052715.

CTW - C.T.W. was supported by NIH/NHGRI (RM1HG011016, UM1HG011593).

SA - S.A., was supported by the NIH/NHGRI through RM1HG011016 (Center for Genome Imaging) and UM1HG011593 (4DN).

ANB - A.N.B. was supported by NIH (U01DK127419)

IF - I.F. was supported by The Giovanni Armenise-Harvard Foundation (Career Development Award, 2022).

CSDC - C.S.D.C. was supported by grant #2021-244318 (5022) awarded to C.S.D.C. by the Chan Zuckerberg Initiative DAF, an advised fund of Silicon Valley Community Foundation, as part of their Imaging Scientist RFA. Major funding also came from NIH grants #U01CA200059-06, #UM1HG011536-04S1 and #U01CA260699.

SW - S.W. was partly supported by NIH (UH3CA268202, U01CA260701, R01HG011245, R33CA251037, DP2GM137414, R01CA292936, R01HG012969, R01HG013503), Pershing Square Sohn Cancer Research Alliance, American Federation for Aging Research and Hevolution Foundation.

Authors Contributions Statement

Author contributions categories utilized here were devised by the CRediT initiative^{123,124}.

Co-first authors (the following authors contributed equally to this work and are listed in alphabetical order)

RN: Conceptualization, Data curation, Methodology, Project administration, Validation, Writing – review & editing

AC: Conceptualization, Data curation, Methodology, Validation, Writing – review & editing

Authors involved in acquiring CT dataset and curating them to be compatible with FOF-CT (these authors contributed equally to this work and are listed in alphabetical order)

BB: Data curation, Experiments / Investigation

YC: Conceptualization, Experiments / Investigation

VG: Data curation, Experiments / Investigation

SG: Data curation, Writing – review & editing

TF: Conceptualization, Data curation, Experiments / Investigation

AH: Data curation, Experiments / Investigation

AJ: Experiments/Investigation, Resources

BBJ: Analysis, Experiments / Investigation, Software

APJ: Conceptualization, Data curation, Experiments / Investigation, Resources

GL: Data curation, Experiments / Investigation

AL: Conceptualization, Validation, Visualization

NMM: Conceptualization, Validation, Visualization, Writing – review & editing

WJM: Conceptualization, Data curation, Software, Validation

YT: Experiments / Investigation, Resources

FW: Conceptualization, Data curation, Validation

KY: Experiments / Investigation

HZ: Experiments / Investigation

QZ: Experiments / Investigation, Methodology, Resources, Writing – review & editing

MB: Funding acquisition, Experiments / Investigation, Writing – review & editing

LB: Conceptualization, Funding acquisition, Experiments / Investigation, Supervision, Writing – review & editing

LC: Funding acquisition, Experiments / Investigation

Principal investigators of FOF-CT publications (these authors contributed equally to this work and are listed in alphabetical order)

BD: Funding acquisition

JRS: Data curation, Funding acquisition, Experiments / Investigation, Writing – review & editing

GV: Conceptualization, Funding acquisition, Methodology, Project administration, Supervision

BR: Funding acquisition, Project administration, Supervision

PPJ: Funding acquisition, Project administration, Supervision

ANS: Data curation, Funding acquisition, Software

AS: Data curation, Project administration, Supervision

JRS: Funding acquisition, Project administration, Supervision, Validation, Writing – review & editing

GV: Data curation, Funding acquisition, Experiments / Investigation

CW: Conceptualization, Funding acquisition, Writing – review & editing

Co-senior authors (the following authors contributed equally to this work and are listed in alphabetical order)

SA: Conceptualization, Methodology, Project administration, Supervision, Validation, Visualization, Writing – original draft, Writing – review & editing

ANB: Conceptualization, Data curation, Experiments / Investigation, Methodology, Writing – original draft, Writing – review & editing

IF: Conceptualization, Funding acquisition, Methodology, Project administration, Software, Supervision, Writing – original draft, Writing – review & editing

CS: Conceptualization, Data curation, Funding acquisition, Methodology, Project administration, Resources, Supervision, Validation, Visualization, Writing – original draft, Writing – review & editing

SW: Conceptualization, Data curation, Analysis, Funding acquisition, Experiments / Investigation, Methodology, Project administration, Resources, Software, Supervision, Validation, Visualization, Writing – original draft, Writing – review & editing

Conflict of Interest Statement

The authors listed below have provided the following conflict of interest statements:

BR - B.R. is a cofounder of Arima Genomics and Epigenome Technologies

CW - The Wu laboratory holds or has patent filings pertaining to imaging and has held a sponsored research agreement with Bruker Inc. CTW is a non-equity-holding co-founder of Acuity Spatial Genomics and, through personal connections to George Church, has equity in companies associated with him.

SA - The Wu laboratory holds or has patent filings pertaining to imaging and has held a sponsored research agreement with Bruker Inc. CTW is a co-founder of Acuity Spatial Genomics and, through personal connections to George Church, has equity in companies associated with him, including 10x Genomics and Twist.

SW - S.W. is a co-inventor on patent applications related to the chromatin tracing technology.

References

1. Dekker, J. *et al.* The 4D nucleome project. *Nature* **549**, 219–226 (2017).
2. Dekker, J. *et al.* Spatial and temporal organization of the genome: Current state and future aims of the 4D nucleome project. *Mol. Cell* **83**, 2624–2640 (2023).
3. 4D Nucleome Consortium *et al.* An integrated view of the structure and function of the human 4D nucleome. *bioRxiv.org* (2024) doi:10.1101/2024.09.17.613111.
4. Fraser James, Williamson Iain, Bickmore Wendy A. & Dostie Josée. An Overview of Genome Organization and How We Got There: from FISH to Hi-C. *Microbiol. Mol. Biol. Rev.* **79**, 347–372 (2015).
5. Jerkovic, I. & Cavalli, G. Understanding 3D genome organization by multidisciplinary methods. *Nat. Rev. Mol. Cell Biol.* **22**, 511–528 (2021).
6. Cremer, T. & Cremer, M. Chromosome territories. *Cold Spring Harb. Perspect. Biol.* **2**, a003889 (2010).
7. Gilbert, N., Gilchrist, S. & Bickmore, W. A. Chromatin organization in the mammalian nucleus. *Int. Rev. Cytol.* **242**, 283–336 (2005).
8. Itzkovitz, S. & van Oudenaarden, A. Validating transcripts with probes and imaging technology. *Nat. Methods* **8**, S12–9 (2011).
9. Levsky, J. M. & Singer, R. H. Fluorescence in situ hybridization: past, present and future. *J. Cell Sci.* **116**, 2833–2838 (2003).
10. Boyle, S., Rodesch, M. J., Halvensleben, H. A., Jeddeloh, J. A. & Bickmore, W. A. Fluorescence in situ hybridization with high-complexity repeat-free oligonucleotide probes generated by massively parallel synthesis. *Chromosome Res.* **19**, 901–909 (2011).
11. Yamada, N. A. *et al.* Visualization of fine-scale genomic structure by oligonucleotide-based high-resolution FISH. *Cytogenet. Genome Res.* **132**, 248–254 (2011).
12. Beliveau, B. J. *et al.* Versatile design and synthesis platform for visualizing genomes with Oligopaint FISH probes. *Proc. Natl. Acad. Sci. U. S. A.* **109**, 21301–21306 (2012).
13. Boettiger, A. & Murphy, S. Advances in Chromatin Imaging at Kilobase-Scale Resolution. *Trends Genet.* **36**, 273–287 (2020).
14. Chen, K. H., Boettiger, A. N., Moffitt, J. R., Wang, S. & Zhuang, X. RNA imaging. Spatially resolved, highly

multiplexed RNA profiling in single cells. *Science* **348**, aaa6090 (2015).

15. Zhuang, X. Spatially resolved single-cell genomics and transcriptomics by imaging. *Nat. Methods* **18**, 18–22 (2021).
16. Bouwman, B. A. M., Crosetto, N. & Bienko, M. The era of 3D and spatial genomics. *Trends Genet.* **38**, 1062–1075 (2022).
17. Flores, V., Farabella, I. & Nir, G. Genome-wide tracing to decipher nuclear organization. *Curr. Opin. Cell Biol.* **82**, 102175 (2023).
18. Hafner, A. & Boettiger, A. The spatial organization of transcriptional control. *Nat. Rev. Genet.* **24**, 53–68 (2023).
19. Yang, T. & Wang, S. Image-based 3D genomics through chromatin tracing. *Nat. Rev. Methods Primers* **4**, (2024).
20. Cardozo Gizzi, A. M. A shift in paradigms: Spatial genomics approaches to reveal single-cell principles of genome organization. *Front. Genet.* **12**, 780822 (2021).
21. Xie, L. & Liu, Z. Single-cell imaging of genome organization and dynamics. *Mol. Syst. Biol.* **17**, e9653 (2021).
22. Mateo, L. J. *et al.* Visualizing DNA folding and RNA in embryos at single-cell resolution. *Nature* **568**, 49–54 (2019).
23. Liu, M. *et al.* Multiplexed imaging of nucleome architectures in single cells of mammalian tissue. *Nat. Commun.* **11**, 2907 (2020).
24. Su, J.-H., Zheng, P., Kinrot, S. S., Bintu, B. & Zhuang, X. Genome-Scale Imaging of the 3D Organization and Transcriptional Activity of Chromatin. *Cell* **182**, 1641–1659.e26 (2020).
25. Hu, M. & Wang, S. Chromatin Tracing: Imaging 3D Genome and Nucleome. *Trends Cell Biol.* **31**, 5–8 (2021).
26. Wang, S. *et al.* Spatial organization of chromatin domains and compartments in single chromosomes. *Science* **353**, 598–602 (2016).
27. Takei, Y. *et al.* Integrated spatial genomics reveals global architecture of single nuclei. *Nature* **590**, 344–350 (2021).
28. Takei, Y. *et al.* Single-cell nuclear architecture across cell types in the mouse brain. *Science* **374**, 586–594 (2021).
29. Cardozo Gizzi, A. M. *et al.* Microscopy-Based Chromosome Conformation Capture Enables Simultaneous Visualization of Genome Organization and Transcription in Intact Organisms. *Mol. Cell* **74**, 212–222.e5 (2019).
30. Rajpurkar, A. R., Mateo, L. J., Murphy, S. E. & Boettiger, A. N. Deep learning connects DNA traces to transcription to reveal predictive features beyond enhancer-promoter contact. *Nat. Commun.* **12**, 3423 (2021).
31. Murphy, S. E. & Boettiger, A. N. Polycomb repression of Hox genes involves spatial feedback but not domain compaction or phase transition. *Nat. Genet.* **56**, 493–504 (2024).

32. Le, D. J., Hafner, A., Gaddam, S., Wang, K. C. & Boettiger, A. N. Super-enhancer interactomes from single cells link clustering and transcription. *bioRxiv* 2024.05.08.593251 (2024) doi:10.1101/2024.05.08.593251.

33. Takei, Y., Shah, S., Harvey, S., Qi, L. S. & Cai, L. Multiplexed Dynamic Imaging of Genomic Loci by Combined CRISPR Imaging and DNA Sequential FISH. *Biophys. J.* **112**, 1773–1776 (2017).

34. Nguyen, H. Q. *et al.* 3D mapping and accelerated super-resolution imaging of the human genome using in situ sequencing. *Nat. Methods* **17**, 822–832 (2020).

35. Payne, A. C. *et al.* In situ genome sequencing resolves DNA sequence and structure in intact biological samples. *Science* **371**, (2021).

36. Llimos, G. *et al.* A leukemia-protective germline variant mediates chromatin module formation via transcription factor nucleation. *Nat. Commun.* **13**, 2042 (2022).

37. Weber, C. M. *et al.* mSWI/SNF promotes Polycomb repression both directly and through genome-wide redistribution. *Nat. Struct. Mol. Biol.* **28**, 501–511 (2021).

38. Chen, L.-F. *et al.* Structural elements promote architectural stripe formation and facilitate ultra-long-range gene regulation at a human disease locus. *Mol. Cell* (2023) doi:10.1016/j.molcel.2023.03.009.

39. Jensen, C. L. *et al.* Long-range regulation of transcription scales with genomic distance in a gene-specific manner. *Mol. Cell* **85**, 347–361.e7 (2025).

40. Espinola, S. M. *et al.* Cis-regulatory chromatin loops arise before TADs and gene activation, and are independent of cell fate during early Drosophila development. *Nat. Genet.* **53**, 477–486 (2021).

41. Sawh, A. N. *et al.* Lamina-dependent stretching and unconventional chromosome compartments in early *C. elegans* embryos. *Mol. Cell* **78**, 96–111.e6 (2020).

42. Huang, Y. *et al.* Two unrelated distal genes activated by a shared enhancer benefit from localizing inside the same small topological domain. *Genes Dev.* **39**, 348–363 (2025).

43. Huang, H. *et al.* CTCF mediates dosage- and sequence-context-dependent transcriptional insulation by forming local chromatin domains. *Nat. Genet.* **53**, 1064–1074 (2021).

44. Hafner, A., Park, M., Berger, S. E., Nora, E. P. & Boettiger, A. N. Loop stacking organizes genome folding from TADs to chromosomes. *Mol. Cell* **83**, (2023).

45. Jay, A. *et al.* Single-Allele Chromatin Tracing Reveals Genomic Clustering of Paralogous Transcription Factors as a

Mechanism for Developmental Robustness in T Cells. *bioRxivorg* (2025) doi:10.1101/2025.05.30.656885v1.

46. Bintu, B. *et al.* Super-resolution chromatin tracing reveals domains and cooperative interactions in single cells. *Science* **362**, eaau1783 (2018).
47. Cheng, Y., Liu, M., Hu, M. & Wang, S. TAD-like single-cell domain structures exist on both active and inactive X chromosomes and persist under epigenetic perturbations. *Genome Biol.* **22**, 309 (2021).
48. Mota, A., Schweitzer, M., Wernersson, E., Crosetto, N. & Bienko, M. Simultaneous visualization of DNA loci in single cells by combinatorial multi-color iFISH. *Sci Data* **9**, 47 (2022).
49. Jia, B. B., Jussila, A., Kern, C., Zhu, Q. & Ren, B. A spatial genome aligner for resolving chromatin architectures from multiplexed DNA FISH. *Nat. Biotechnol.* **41**, 1004–1017 (2023).
50. Hung, T.-C., Kingsley, D. M. & Boettiger, A. N. Nat Met_Boundary stacking interactions enable cross-TAD enhancer-promoter communication during limb development. *Nat. Genet.* **56**, 306–314 (2024).
51. Patterson, B. *et al.* Female naïve human pluripotent stem cells carry X chromosomes with Xa-like and Xi-like folding conformations. *Sci. Adv.* **9**, eadf2245 (2023).
52. Messina, O. *et al.* 3D chromatin interactions involving Drosophila insulators are infrequent but preferential and arise before TADs and transcription. *Nat. Commun.* **14**, 6678 (2023).
53. Tastemel, M. *et al.* Context-dependent and gene-specific role of chromatin architecture mediated by histone modifiers and loop-extrusion machinery. *bioRxivorg* (2025) doi:10.1101/2025.02.21.639596.
54. Gutnik, S., You, J. E., Sawh, A. N., Andriollo, A. & Mango, S. E. Multiplex DNA fluorescence in situ hybridization to analyze maternal vs. paternal *C. elegans* chromosomes. *Genome Biol.* **25**, 71 (2024).
55. Liu, M. *et al.* Tracing the evolution of single-cell cancer 3D genomes: an atlas for cancer gene discovery. *bioRxiv* (2024).
56. Fujimori, T. *et al.* Single-cell chromatin state transitions during epigenetic memory formation. *bioRxivorg* (2023) doi:10.1101/2023.10.03.560616.
57. Cheng, Y. *et al.* Perturb-tracing enables high-content screening of multiscale 3D genome regulators. *bioRxivorg* (2023) doi:10.1101/2023.01.31.525983.
58. Liu, S. *et al.* Sci Adv_Cell type-specific 3D-genome organization and transcription regulation in the brain. *Sci. Adv.* **11**, eadv2067 (2025).

59. Beliveau, B. J. *et al.* In Situ Super-Resolution Imaging of Genomic DNA with OligoSTORM and OligoDNA-PAINT. *Methods Mol. Biol.* **1663**, 231–252 (2017).

60. Nir, G. *et al.* Walking along chromosomes with super-resolution imaging, contact maps, and integrative modeling. *PLoS Genet.* **14**, e1007872 (2018).

61. Luppino, J. M. *et al.* Cohesin promotes stochastic domain intermingling to ensure proper regulation of boundary-proximal genes. *Nat. Genet.* **52**, 840–848 (2020).

62. Beliveau, B. J. *et al.* Single-molecule super-resolution imaging of chromosomes and in situ haplotype visualization using Oligopaint FISH probes. *Nat. Commun.* **6**, 7147 (2015).

63. Boettiger, A. N. *et al.* Super-resolution imaging reveals distinct chromatin folding for different epigenetic states. *Nature* **529**, 418–422 (2016).

64. Kempfer, R. & Pombo, A. Methods for mapping 3D chromosome architecture. *Nat. Rev. Genet.* **21**, 207–226 (2020).

65. Gholamalamdari, O. *et al.* Major nuclear locales define nuclear genome organization and function beyond A and B compartments. *Elife* **13**, (2025).

66. Kraft, K. *et al.* Polycomb-mediated genome architecture enables long-range spreading of H3K27 methylation. *Proc. Natl. Acad. Sci. U. S. A.* **119**, e2201883119 (2022).

67. Hung, T.-C., Kingsley, D. M. & Boettiger, A. Boundary stacking interactions enable cross-TAD enhancer-promoter communication during limb development. *bioRxiv* 2023.02.06.527380 (2023) doi:10.1101/2023.02.06.527380.

68. Willemijn, A., Szabó, D. & Pombo, A. Epigenetic regulatory layers in the 3D nucleus. *Mol. Cell* **84**, 415–428 (2024).

69. Farabella, I., Di Stefano, M., Soler-Vila, P., Martí-Marimon, M. & Martí-Renom, M. A. Three-dimensional genome organization via triplex-forming RNAs. *Nat. Struct. Mol. Biol.* **28**, 945–954 (2021).

70. Takei, Y. *et al.* Spatial multi-omics reveals cell-type-specific nuclear compartments. *Nature* **641**, 1037–1047 (2025).

71. Gurgo, J. *et al.* Multiplexed chromatin imaging reveals predominantly pairwise long-range coordination between Drosophila Polycomb genes. *Cell Rep.* **43**, 114167 (2024).

72. Götz, M., Messina, O., Espinola, S., Fiche, J.-B. & Nollmann, M. Multiple parameters shape the 3D chromatin structure of single nuclei at the doc locus in Drosophila. *Nat. Commun.* **13**, 5375 (2022).

73. van Steensel, B. & Belmont, A. S. Lamina-associated domains: Links with chromosome architecture, heterochromatin, and gene repression. *Cell* **169**, 780–791 (2017).

74. Bohrer, C. H. & Larson, D. R. Synthetic analysis of chromatin tracing and live-cell imaging indicates pervasive spatial coupling between genes. *Elife* **12**, (2023).

75. Goundaroulis, D., Lieberman Aiden, E. & Stasiak, A. Chromatin is frequently unknotted at the megabase scale. *Biophys. J.* **118**, 2268–2279 (2020).

76. Patel, R., Pham, K., Chandrashekhar, H. & Phillips-Cremins, J. E. FISHnet: Detecting chromatin domains in single-cell sequential Oligopaints imaging data. *Molecular Biology* (2024).

77. Liefsoens, M., Földes, T. & Barbi, M. Spectral-based detection of chromatin loops in multiplexed super-resolution FISH data. *Nat. Commun.* **15**, 7670 (2024).

78. Wang, H. *et al.* Tensor-FLAMINGO unravels the complexity of single-cell spatial architectures of genomes at high-resolution. *Nat. Commun.* **16**, 3435 (2025).

79. Conte, M. *et al.* Loop-extrusion and polymer phase-separation can co-exist at the single-molecule level to shape chromatin folding. *Nat. Commun.* **13**, 4070 (2022).

80. Conte, M. *et al.* Polymer physics indicates chromatin folding variability across single-cells results from state degeneracy in phase separation. *Nat. Commun.* **11**, 3289 (2020).

81. Fiorillo, L. *et al.* Comparison of the Hi-C, GAM and SPRITE methods using polymer models of chromatin. *Nat. Methods* **18**, 482–490 (2021).

82. Castillo, D., Mendieta-Esteban, J. & Marti-Renom, M. A. Probabilistic 3D-modelling of genomes and genomic domains by integrating high-throughput imaging and Hi-C using machine learning. *bioRxiv* (2022) doi:10.1101/2022.09.19.508575v1.

83. Wang, H., Yang, J., Zhang, Y., Qian, J. & Wang, J. Reconstruct high-resolution 3D genome structures for diverse cell-types using FLAMINGO. *Nat. Commun.* **13**, 2645 (2022).

84. Zhang, R., Zhou, T. & Ma, J. Multiscale and integrative single-cell Hi-C analysis with Higashi. *Nat. Biotechnol.* **40**, 254–261 (2022).

85. Remini, L. *et al.* Chromatin structure from high resolution microscopy: Scaling laws and microphase separation. *Phys. Rev. E.* **109**, 024408 (2024).

86. Remini, L., Segers, M., Parmeggiani, A. & Carlon, E. Inferring interphase chromosomal structure from multiplexed fluorescence in situ hybridization data: A unified picture from human and mouse cells. *J. Chem. Phys.* **162**, (2025).

87. Zhang, Y. *et al.* Computational methods for analysing multiscale 3D genome organization. *Nat. Rev. Genet.* (2023) doi:10.1038/s41576-023-00638-1.

88. Boninsegna, L. *et al.* Integrative genome modeling platform reveals essentiality of rare contact events in 3D genome organizations. *Nat. Methods* **19**, 938–949 (2022).

89. Hammer, M. *et al.* Towards community-driven metadata standards for light microscopy: tiered specifications extending the OME model. *Nature Methods* **18**, 1427–1440 (2021).

90. Rigano, A. *et al.* Micro-Meta App: an interactive tool for collecting microscopy metadata based on community specifications. *Nat. Methods* **18**, 1489–1495 (2021).

91. Cosolo, A. *et al.* 4DN FISH omics format - Chromatin Tracing (FOF-CT). *ReadTheDocs* <https://fish-omics-format.readthedocs.io/en/latest/> (2021).

92. Niu, J., Denisko, D. & Hoffman, M. M. The Browser Extensible Data (BED) format. *SAM/BAM and related specifications* (2022).

93. Global Alliance for Genomics & Health (GA4GH). *The Variant Call Format Specification*. <https://samtools.github.io/hts-specs/VCFv4.5.pdf> (2024).

94. Reiff, S. B. *et al.* The 4D Nucleome Data Portal as a resource for searching and visualizing curated nucleomics data. *Nat. Commun.* **13**, 2365 (2022).

95. Strambio-De-Castillia, C. & Rigano, A. Micro-Meta App: Microscopy Metadata for the real world! *Micro-Meta App Website* <https://wu-bimac.github.io/MicroMetaApp.github.io/> (2020).

96. Devos, X. *et al.* pyHiM: a new open-source, multi-platform software package for spatial genomics based on multiplexed DNA-FISH imaging. *Genome Biol.* **25**, 47 (2024).

97. Nollmann, M. & Devos, X. *Traceratops Documentation — Traceratops 0.5.0 Documentation*. <https://traceratops.readthedocs.io/en/main> (2025).

98. Williams, E. *et al.* The Image Data Resource: A Bioimage Data Integration and Publication Platform. *Nat. Methods* **14**, 775–781 (2017).

99. Ross, B. C. & Wiggins, P. A. Measuring chromosome conformation with degenerate labels. *Phys. Rev. E Stat. Nonlin. Soft Matter Phys.* **86**, 011918 (2012).

100. Lee, L. *et al.* SnapFISH: a computational pipeline to identify chromatin loops from multiplexed DNA FISH data.

Nat. Commun. **14**, 4873 (2023).

101. Huang, L. O. *et al.* Genome-wide discovery of genetic loci that uncouple excess adiposity from its comorbidities. *Nat Metab* **3**, 228–243 (2021).
102. Yu, H. *et al.* Accurate and robust 3D genome feature discovery from multiplexed DNA FISH. *BioArXiv* (2025) doi:10.1101/2025.11.26.690837v1.
103. Yu, H. *et al.* SnapFISH-IMPUTE: an imputation method for multiplexed DNA FISH data. *Commun. Biol.* **7**, 834 (2024).
104. Fan, S., Dang, D., Gao, L. & Zhang, S. ImputeHiFI: An imputation method for multiplexed DNA FISH data by utilizing single-cell Hi-C and RNA FISH data. *Adv. Sci. (Weinh.)* **11**, e2406364 (2024).
105. Zhu, X. *et al.* Nucleome Browser: an integrative and multimodal data navigation platform for 4D Nucleome. *Nat. Methods* **19**, 911–913 (2022).
106. Wellcome Trust Sanger Institute. FASTQ Format. *Maq (Mapping and Assembly with Qualities) Sourceforge* <https://maq.sourceforge.net/fastq.shtml>.
107. Global Alliance for Genomics & Health (GA4GH). Sequence Alignment/Map Format Specification. *SAM/BAM and related specifications* (2022).
108. GA4GH Consortium. *Global Alliance for Genomics and Health (GA4GH) 2020-2021 Strategic Plan*. <https://www.ga4gh.org/document/strategic-roadmap-2020/> (2021).
109. Davis, C. A. *et al.* The Encyclopedia of DNA elements (ENCODE): data portal update. *Nucleic Acids Res.* **46**, D794–D801 (2018).
110. Yilmaz, V., Abdennur, N. & Open Chromosome Collective. Open2C: Advancing 3D and functional genomics research. (2024) doi:10.7490/f1000research.1120066.1.
111. wwPDB consortium. Protein Data Bank: the single global archive for 3D macromolecular structure data. *Nucleic Acids Res.* **47**, D520–D528 (2019).
112. Deutsch, E. W. File formats commonly used in mass spectrometry proteomics. *Mol. Cell. Proteomics* **11**, 1612–1621 (2012).
113. The Nobel Prize in Chemistry 2024. *NobelPrize.org* <https://www.nobelprize.org/prizes/chemistry/2024/summary/>.
114. Beckwith, K. S., Brunner, A., Morero, N. R., Jungmann, R. & Ellenberg, J. Nanoscale 3D DNA tracing reveals the

mechanism of self-organization of mitotic chromosomes. *bioRxiv.org* (2024) doi:10.1101/2024.10.28.620625.

115. Beckwith, K. S., Brunner, A., Morero, N. R., Jungmann, R. & Ellenberg, J. Nanoscale DNA tracing reveals the self-organization mechanism of mitotic chromosomes. *Cell* **188**, 2656–2669.e17 (2025).

116. Beckwith, K. S. *et al.* Nanoscale 3D DNA tracing in single human cells visualizes loop extrusion directly *in situ* - version 5. *bioRxiv* (2023) doi:10.1101/2021.04.12.439407.

117. Wang, Y. *et al.* Genome oligopaint via local denaturation fluorescence *in situ* hybridization. *Mol. Cell* **81**, 1566–1577.e8 (2021).

118. Steinek, C. *et al.* Generation of densely labeled oligonucleotides for the detection of small genomic elements. *Cell Rep. Methods* **4**, 100840 (2024).

119. Yang, L. *et al.* (Tn5-)FISH-based imaging in the era of 3D/spatial genomics. *Biophys. Rep.* **9**, 15–25 (2023).

120. Mota, A. *et al.* FRET-FISH probes chromatin compaction at individual genomic loci in single cells. *Nat. Commun.* **13**, 6680 (2022).

121. Wilkinson, M. D. *et al.* The FAIR Guiding Principles for scientific data management and stewardship. *Sci Data* **3**, 160018 (2016).

122. Marconato, L. *et al.* SpatialData: an open and universal data framework for spatial omics. *Nat. Methods* **22**, 58–62 (2025).

123. Allen, L., O'Connell, A. & Kiermer, V. How can we ensure visibility and diversity in research contributions? How the Contributor Role Taxonomy (CRediT) is helping the shift from authorship to contributorship. *Learn. Publ.* **32**, 71–74 (2019).

124. Elsevier editors. CRediT author statement - editorial. *Elsevier* (<https://www.elsevier.com/authors/policies-and-guidelines/credit-author-statement>) (2020).

Figures

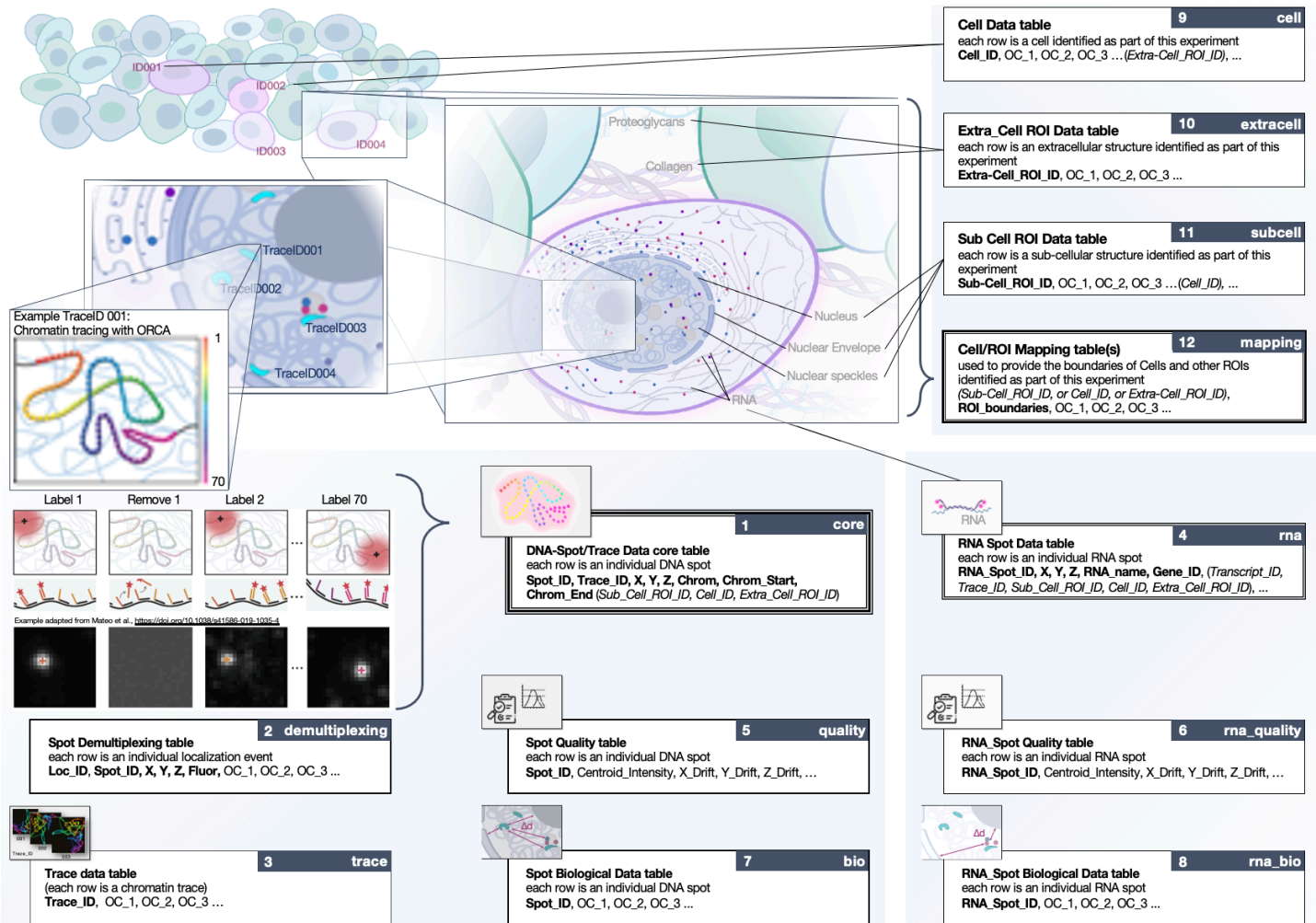


Figure 1: Schematic Representation of the 12 tables comprising the FISH Omics Format for Chromatin Tracing. The FISH Omics Format for Chromatin Tracing (FOF-CT) format consists of 12 individual tables capturing different aspects of Chromatin Tracing data. A full description of the format can be found on ReadTheDocs (https://github.com/4dn-dcic/fish_omics_format). Displayed here is a summary in which individual tables are represented as boxes whose number and short name is indicated in the upper right corner of the box. The core of the format is the DNA-Spot table (1 core), which defines chromatin traces as ensembles of individual DNA-FISH bright Spots (Supplemental Table I - Glossary). Additional tables support the integration of this core information with complementary data, including raw data (2), trace information (3), quality metrics (5), and physical coordinates to place Spots/Traces within the cellular context (7, 10, 11, 12). The format also accommodates multiplexed RNA-FISH results (4, 6, 8). Submitting a dataset requires the core Spot table, while additional quality metrics and biological properties associated with individual Spots are recommended. Demultiplexing and trace information are optional, and all other tables are conditionally necessary depending on the experiment.

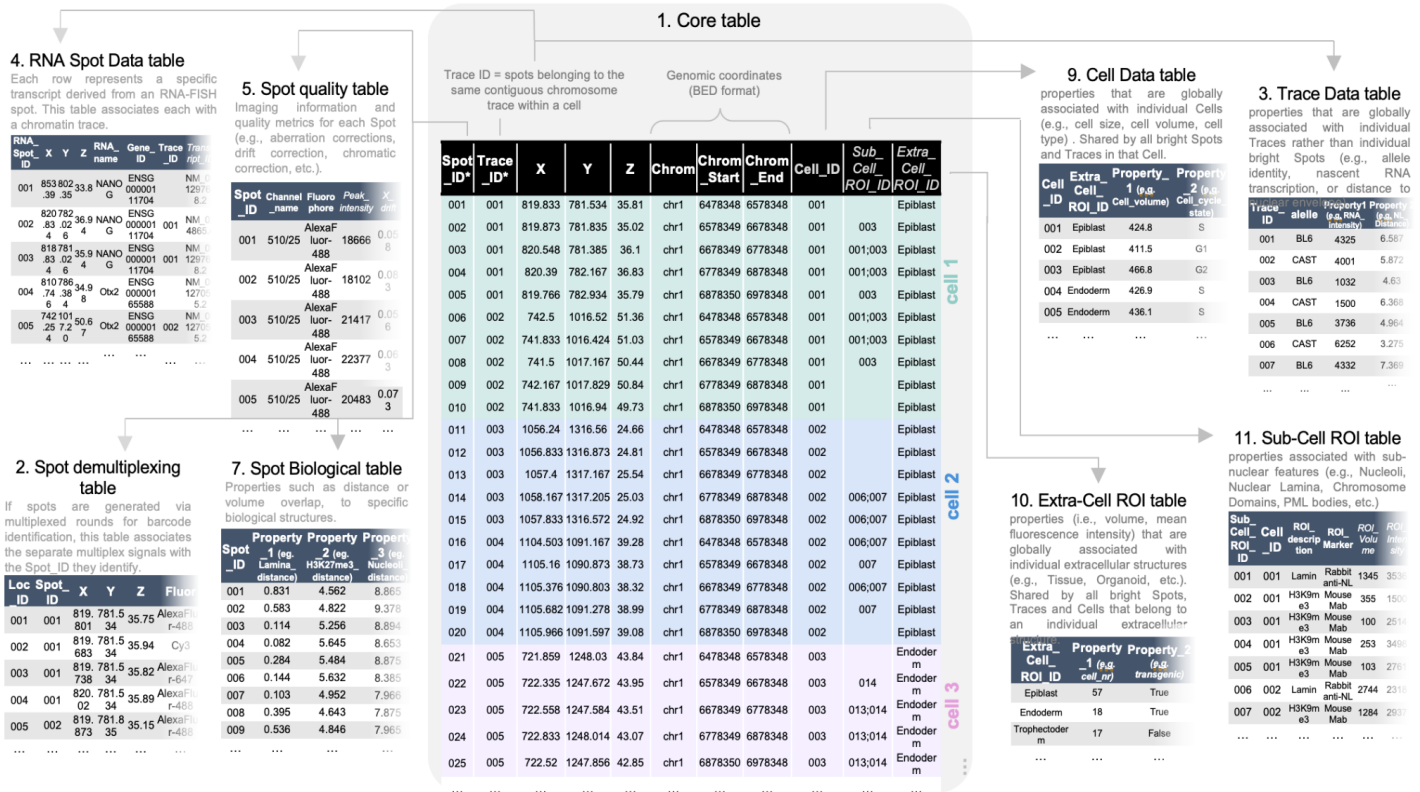


Figure 2. Anatomy of the Core FOF-CT table and connection to other data tables. An example of a *Core Table*, with the first 5 traces corresponding to 3 cells, is shown. Examples of additional tables are shown as well, connected to the Core table by a corresponding variable column (e.g., Spot_ID connects the Spot quality table to the Core table, and Cell_ID connects the Sub-Cell ROI table to the Core table). Only the top few rows of each example table are shown (table data will continue further below). Mandatory columns are shown with their name in bold, and optional columns are shown in italicics.

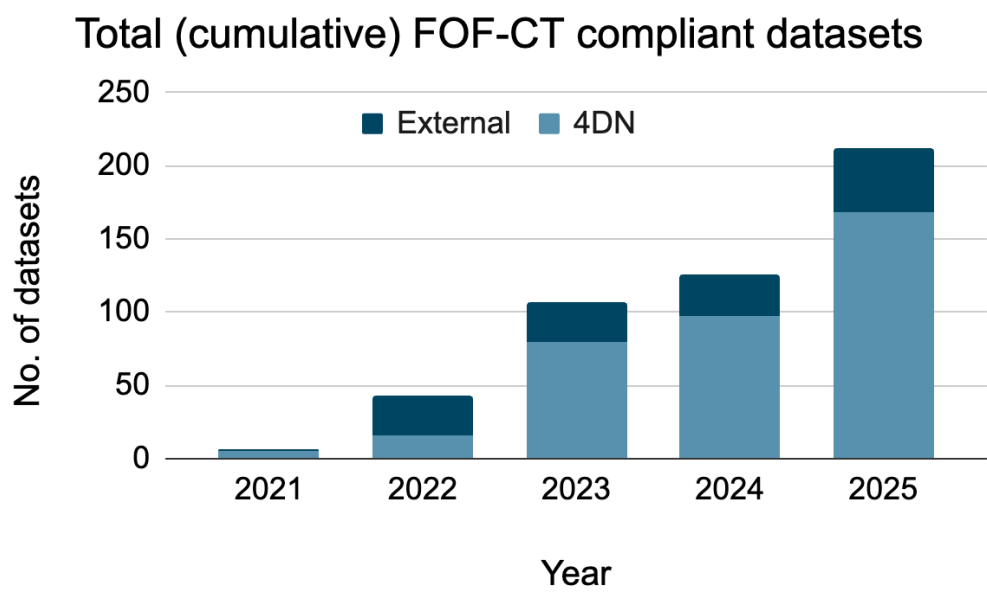
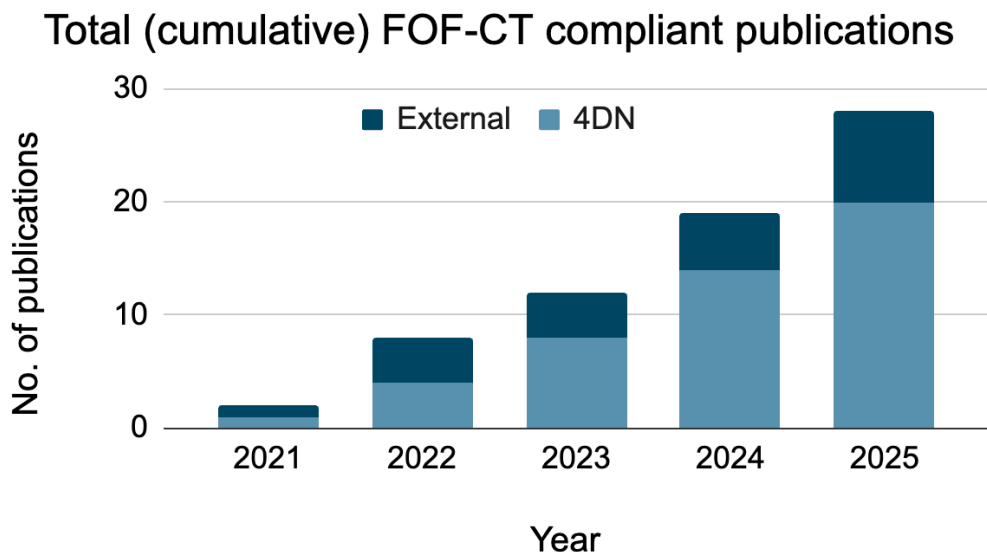


Figure 3. Adoption and impact of the FOF-CT standard on publicly available datasets and publications. Since its introduction, the FOF-CT standard has driven a substantial increase in compliant datasets and publications (Supplemental Table II) deposited in the 4DN Data Portal and the Image Data Resource (IDR) from both laboratories that belonged to the 4DN consortium (*light blue*) or were External to it (*dark blue*), demonstrating broad community adoption. (*Top*) Number of FOF-CT-compliant publications available through the 4DN Data Portal ($n = 27$) and the IDR ($n = 1$; project link: [IDR project 2251]) for a total of 28 publications. (*Bottom*) Number of deposited FOF-CT-compliant datasets in the 4DN Data Portal ($n = 203$) and the IDR ($n = 9$; project link: [IDR project 2251]) for a total of 212 datasets. *Note:* Jia et al., 2022 did not generate new datasets but re-analyzed data from Takei et al., 2021 (*Nature*) and Takei et al., 2021 (*Science*).

Supplemental Material

The following Supplemental Material is available with this publication.

Supplemental Table I - Glossary of Terms

List of terms used in the main text and their description. Abbreviations: BED, Browser Extensible Data; CT, Chromatin Tracing; BS, Backstreet; MS, Mainstreet.

Supplemental Table II: List of FOF-CT compatible datasets and publications that are publicly available on the 4DN Data Portal and IDR

Detailed summary of FOF-CT compatible publications and associated datasets that are made available to the public as part of this publication.

Supplemental Table III: Community-driven microscopy Metadata specifications compliant Hardware description of the microscopes used to produce published FOF-CT publications and datasets

Location on the 4DN Data Portal of the Microscope-Hardware JSON file(s) describing the 4DN-BINA-OME-QUAREP (NBO-Q) Microscopy Metadata specifications^{89,90} compliant configurations of the microscopes used to produce the indicated datasets. These Microscope JSON files were produced using the Micro-Meta App software and can be viewed and compared on the 4DN Data Portal using the Micro-Meta App user interface.

Supplemental Table I: Glossary of Terms

Name	Description	Alternative names
Targeted Region	A genomic region that is targeted for imaging-based analysis	Locus, DNA region
Targeted Segment	A segment of genomic DNA or RNA transcript into which the Targeted Region is subdivided to enable imaging-based analysis. The size of the Targeted Segment often determines the genomic resolution of the analysis.	DNA region, RNA sequence, chromosomal segment
Oligo Target	This is the target sequence for the Target-Specific Oligo. The list of Oligo Target sequences are typically stored in a BED file and are used to construct the oligo library. Thus if the library has 1000 unique Target-Specific Oligos, there would be 1000 unique OligoTarget sequences.	
Targeting Oligo Sequence	This is the section of the Target-Specific Oligo sequence that anneals to the Oligo Target.	Target Annealing Sequence; Region of homology to the DNA or RNA target, genome homology region.
Target-Specific Oligo	This oligonucleotide binds to a unique Oligo Target sequence and is typically made up of three parts: (1) Targeting Sequence – located in the center, complementary to the target. (2) Mainstreet Oligo Sequences (MS) – one or more sequences positioned upstream (5' side) of the Targeting Oligo Sequence. These are usually named, from 5' to 3': Universal MS (UMS), MS1, MS2. (3) Backstreet Oligo Sequences (BS) – one or more sequences positioned downstream (3' side) of the Oligo Targeting Sequence. These are usually named, from 3' to 5': Universal BS (UBS), BS1, BS2.	Oligopaint oligo
Multiplexed-FISH Probe	This is the pool of multiple (i.e., dozens to thousands) individual Target-Specific Oligos, which when combined in a Chromatin Tracing (CT) experiment allow a Targeted Segment to be identified univocally and detected.	
Single-molecule localization	The sub-pixel localization of each detected emission event of a single-molecule fluorophore.	
Spot	The centroid fitting of the imaged Spot of a detected fluorescence signal. In ball-and-stick CT imaged Spots reflect the totality of detected fluorescent signal from multiple individual fluorescence-emitting molecules (i.e., fluorophores). Thus in ball-and-stick CT "there is an actual correspondence between the number of targeted genomic segments and the number of imaged spots."	Imaged spot, bright spot, DNA/RNA spot
Localization cloud	A cluster of single-molecule localizations, each representing the fluorescence signal emitted by an individual fluorophore. For example, in volumetric CT, single-molecule localizations from fluorophores bound to target-specific oligos directed against the same targeted segment are grouped into a single localization cloud. Such clouds can contain anywhere from tens to thousands of individual localizations, enabling computation and analysis of the occupied volumes and overlap fractions at each step.	Localization cluster

Legend: List of terms used in the main text and their description. Abbreviations: BED, Browser Extensible Data; CT, Chromatin Tracing; BS, Backstreet; MS, Mainstreet.

Table II: List of FOF-CT compatible datasets and publications that are publicly available on the 4DN Data Portal and IDR

Nr. Reference	DOI	# of FOF-CT Datasets	FOF-CT Experiment Sets URL	FISH Omics Data Type	FISH Omics Technique	Biological sample (organism)	Target cell/tissue (specimen)	Target chromosome	Main Target molecule (RNA, DNA, Proteins)	Notes
1 Wang, S. et al. Spatial organization of chromatin domains and compartments in single chromosomes. <i>Science</i> 353, 598–602 (2016).	https://doi.org/10.1126/science.aaf8084	5	https://data.4dnucleome.org/publications/6162d287-5782-4f40-aacd-d5da75f0770/#expsets-table	ball-and-stick; CT	ball-and-stick; chromatin tracing	H. sapiens	IMR90	Chr20, Chr21, Chr22, and ChrX	DNA	
2 Bintu, B. et al. Super-resolution chromatin tracing reveals domains and cooperative interactions in single cells. <i>Science</i> 362, (2018).	https://doi.org/10.1126/science.aau1783	10	https://data.4dnucleome.org/publications/e6451832-8312-4e74-bd74-742801f726a1/#expsets-table	ball-and-stick; CT	ball-and-stick; chromatin tracing	H. sapiens	IMR90, K562, A549, HCT116	Chr21	DNA	
3 Mateo, L. J. et al. Visualizing DNA folding and RNA in embryos at single-cell resolution. <i>Nature</i> 568, 49–54 (2019).	https://doi.org/10.1038/s41586-019-1035-4	7	https://data.4dnucleome.org/publications/6c007db6-3eba-41d8-9d50-c7e7c05841f/#expsets-table	ball-and-stick; CT	Optical Reconstruction of Chromatin	D. melanogaster, M. musculus	embryo; mESC	dm3[bithorax complex (BX-C);	DNA	
4 Liu, M. et al. Multiplexed imaging of nucleome architectures in single cells of mammalian tissue. <i>Nat. Commun.</i> 11, 2907 (2020).	https://doi.org/10.1038/s41467-020-16732-5	1	https://data.4dnucleome.org/publications/fc5e1d2a-39e9-4c37-8fba-e077532bca74/#expsets-table	ball-and-stick; CT	Multiplexed Imaging of Nucleome	M. musculus	fetal liver tissue sections	mmChr19	DNA	
5 Sawh, A. N. et al. Lamina-dependent stretching and unconventional chromosome compartments in early C. elegans embryos. <i>Mol. Cell</i> 78, 96–111.e6 (2020).	https://doi.org/10.1016/j.molcel.2020.02.006	7	https://data.4dnucleome.org/publications/996fc79a-65e1-4527-9e7b-4089d97511/#expsets-table	ball-and-stick; CT	ball-and-stick; chromatin tracing	C. elegans	embryo 2-40-cells	ceChr5, ceChr1	DNA	
6 Su, J.-H., Zheng, P., Kirrot, S. S., Bintu, B. & Zhuang, X. Genome-Scale Imaging of the 3D Organization and Transcriptional Activity of Chromatin. <i>Cell</i> 182, 1641–1659.e26 (2020).	https://doi.org/10.1010/cell.2020.07.032	3	https://data.4dnucleome.org/publications/bd2062a-7c4c-4a95-9721-e80181da2d4/#expsets-table	ball-and-stick; CT	High-resolution; DNA-MERFISH	H. sapiens	IMR90	High-resolution	DNA, RNA, Proteins	
7 Cheng, Y., Lu, M., Hu, M. & Wang, S. TAD-like single-cell domain structures exist on both active and inactive X chromosomes and persist under epigenetic perturbations. <i>Genome Biol.</i> 22, 309 (2021).	https://doi.org/10.1186/s13059-021-02523-8	9	https://data.4dnucleome.org/publications/9c1ed2e4-0c1d-48c1-85fb-a1b5d5a6dbb8/#expsets-table	ball-and-stick; CT	ball-and-stick; chromatin tracing	H. sapiens	IMR90, H1ERT-RPE1	Active and Inactive X Chromosomes	DNA	
8 Huang, H. et al. CTCF mediates dosage- and sequence-context-dependent transcriptional insulation by forming local chromatin domains. <i>Nat. Genet.</i> 53, 1064–1074 (2021).	https://doi.org/10.1038/s41588-021-00863-6	5	https://data.4dnucleome.org/publications/4f766397-5ead-416e-b891-1c95391dc077/#expsets-table	ball-and-stick; CT	multiplexed FISH	M. musculus	mouse Embryonic Stem Cell	mmChr3	DNA	
9 Takei, Y. et al. Integrated spatial genomics reveals global architecture of single nuclei. <i>Nature</i> 590, 344–350 (2021).	https://doi.org/10.1038/s41586-020-03126-2	1	https://data.4dnucleome.org/publications/745502f5-4f9b-41f5-af4-a89e5d317e58/#expsets-table	ball-and-stick; CT	DNA Sequential Fluorescence In Situ	M. musculus	mESC	mmChr1-19, ChrX	DNA, RNA, Proteins	
10 Takei, Y. et al. Single-cell nuclear architecture across cell types in the mouse brain. <i>Science</i> 374, 586–594 (2021).	https://doi.org/10.1126/science.ab11966	1	https://data.4dnucleome.org/publications/e01653aa-2783-458a-89c5-bc2da572c98/#expsets-table	ball-and-stick; CT	DNA Sequential Fluorescence In Situ	M. musculus	brain	mmChr1-19, ChrX	DNA, RNA, Proteins	
11 Llimos, G. et al. A leukemia-protective germline variant mediates chromatin module formation via transcription factor nucleation. <i>Nat. Commun.</i> 13, 2042 (2022).	https://doi.org/10.1038/s41467-022-29625-6	2	https://data.4dnucleome.org/publications/b874200-5443-4601-91c1-2109227caff/#expsets-table	ball-and-stick; CT	ORCA	H. sapiens	homozygous REF (GM12822)	Chr17	DNA	
12 Mota, A., Schwellert, M., Wernersson, E., Crosetto, N. & Bienko, M. Simultaneous visualization of DNA loci in single cells by combinatorial multi-color IFISH. <i>Sci Data</i> 9, 47 (2022).	https://doi.org/10.1038/s41597-022-01139-2	9	http://idr.openmicroscopy.org/webclient/?show=project-2251	Single-allele pair-wise distance	miFISH	H. sapiens	RPE	Chr1, Chr2, Chr10	DNA	#
13 Jia, B. B., Jussila, A., Kern, C., Zhu, Q. & Ren, B. A spatial genome aligner for resolving chromatin architectures from multiplexed DNA FISH. <i>Nat. Biotechnol.</i> 41, 1004–1017 (2023).	https://doi.org/10.1038/s41587-022-01568-9	* not applicable	https://data.4dnucleome.org/publications/04e04160-bbda-4e5b-8d34-3e99-8f460e97/#expsets-table	* not applicable	re-analysis of published FOF-CT datasets	0	n/a	n/a	n/a	
14 Murphy, S. E. & Boettiger, A. N. Polycomb repression of Hox genes involves spatial feedback but not domain compaction or phase transition. <i>Nat. Genet.</i> 56, 493–504 (2024).	https://doi.org/10.1038/s41588-024-01661-6	5	https://data.4dnucleome.org/publications/17cd0dc6-562c-49ad-beca-0101c0f8c1dc/#expsets-table	ball-and-stick; CT	ORCA	M. musculus	embryonic brain tissue, ESCs, embryonic	mmChr6	DNA, RNA	
15 Hafner, A. et al. Loop stacking organizes genome folding from TADs to chromosomes. <i>Mol. Cell</i> 83, 1377–1392.e6 (2023).	https://doi.org/10.1016/j.molcel.2023.04.008	33	https://data.4dnucleome.org/publications/14334f46-792e-4ec8-b966-206a0b1d5f0/#expsets-table	ball-and-stick; CT	ORCA	M. musculus	mESCs, mESCs depleted of CTCF, mESCs	mmChr3, mmChr 6	DNA, RNA, Proteins	
16 Chen, L.-F. et al. Structural elements promote architectural stripe formation and facilitate ultra-long-range gene regulation at a human disease locus. <i>Mol. Cell</i> 83, 1446–1461.e6 (2023).	https://doi.org/10.1016/j.molcel.2023.03.009	5	https://data.4dnucleome.org/publications/8d89b44d-1fae-447f-8115-6a93eda5919d/#expsets-table	ball-and-stick; CT	ORCA	H. sapiens	H9 hESCs diff to CNCCs	Chr17	DNA, protein	
17 Hung, T.-C., Kingsley, D. M. & Boettiger, A. N. Boundary stacking interactions enable cross-TAD enhancer-promoter communication during limb development. <i>Nat. Genet.</i> 56, 306–314 (2024).	https://doi.org/10.1038/s41588-023-01641-2	1	https://data.4dnucleome.org/publications/3a910b15-f5f7-4684-b2a5-eb212baaeccbb/#expsets-table	ball-and-stick; CT	ORCA	M. musculus	embryonic limbs	mmChr13	DNA	
18 Patterson, B. et al. Female naïve human pluripotent stem cells carry X chromosomes with Xa-like and Xi-like folding conformations. <i>Sci. Adv.</i> 9, eadf2245 (2023).	https://doi.org/10.1126/sciadv.adf2245	21	https://data.4dnucleome.org/publications/2fab6d6e-0c82-4c4d-872d-9e69af521936/#expsets-table	ball-and-stick; CT	ball-and-stick; chromatin tracing	H. sapiens	HPSC	ChrX	DNA	
19 Liu, S. et al. Cell type-specific 3D genome organization and transcription regulation in the brain. <i>Sci. Adv.</i> 11, eadv2067 (2025).	https://doi.org/10.1126/sciadv.adv2067	3	https://data.4dnucleome.org/publications/de7e2893-e23f-4331-899f-889e267e3a9/#expsets-table	ball-and-stick; CT	DNA and RNA MERFISH	M. musculus	mouse brain (RNA MERFISH)	whole genome	DNA, RNA	
20 Messina, O. et al. 3D chromatin interactions involving Drosophila insulators are infrequent but preferential and arise before TADs and transcription. <i>Nat. Commun.</i> 14, 6678 (2023).	https://doi.org/10.1038/s41416-023-02485-5	2	https://data.4dnucleome.org/publications/52fc166-6004-47c0-8590-b44-787a89fe/#expsets-table	ball-and-stick; CT	Hi-M	D. Melanogaster	Nuclear-cycle 14 embryos	dmChr2	DNA	^
21 Tastemel, M. et al. Context-dependent and gene-specific role of chromatin architecture mediated by histone modifiers and loop-extrusion machinery. <i>bioRxiv</i> (2025).	https://doi.org/10.1126/sciadv.adf2245	11	https://data.4dnucleome.org/publications/7b338c4e-a510-41ff-b65a-3891e270c97/#expsets-table	ball-and-stick; CT	ball-and-stick; chromatin tracing	M. musculus	F123-CASTx129 with Sox2 tags	mmChr3	DNA, RNA	
22 Le, D. J. et al. Super-enhancer interactomes from single cells link clustering and transcription. <i>bioRxiv</i> (2024).	https://doi.org/10.1126/sciadv.adf2245	2	https://data.4dnucleome.org/publications/805bb891-8958-4221-941d-d3be90a109e0/#expsets-table	ball-and-stick; CT	ball-and-stick; chromatin tracing	M. musculus	ES-E14TG2a	multiple	DNA	
23 Jensen, C. L. et al. Long-range regulation of transcription scales with genomic distance in a gene-specific manner. <i>Mol. Cell</i> 85, 347–361.e7 (2025).	https://doi.org/10.1016/j.molcel.2024.01.021	3	https://data.4dnucleome.org/publications/0a8a0fd-eafe-44f3-b7a4-7445a09a9816/#expsets-table	ball-and-stick; CT	ball-and-stick; chromatin tracing	M. musculus	R1 mESCs	mmChr5	DNA	
24 Gutnik, S. et al. Multiplex DNA fluorescence in situ hybridization to analyze maternal vs. paternal C. elegans chromosomes. <i>Genome Biol.</i> 25, 71 (2024).	https://doi.org/10.1186/s13059-024-03199-6	6	https://data.4dnucleome.org/publications/1453b156-6de5-438d-b41a-6ff53f5f57b/#expsets-table	ball-and-stick; CT	ball-and-stick; chromatin tracing	C. elegans	embryo 2-40-cells	chr5	DNA	
25 Jay, A. et al. Single-allele chromatin tracing reveals genomic clustering of paralogous transcription factors as a mechanism for developmental robustness in T cells. <i>bioRxiv</i> (2025).	https://doi.org/10.1126/sciadv.adf2245	1	https://data.4dnucleome.org/publications/ebc8c69e-3e8b-477f-b7e6-0d7e75a188f4/#expsets-table	ball-and-stick; CT	ORCA	M. musculus	Double-positive T cells	chr9	DNA	
26 Liu, M. et al. Tracing the evolution of single-cell cancer 3D genomes: an atlas for cancer gene discovery. <i>bioRxiv</i> (2024).	https://doi.org/10.1126/sciadv.adf2245	22	https://data.4dnucleome.org/publications/e83173f1-95e4-40ad-9748-e13b24515f6/#expsets-table	ball-and-stick; CT	ball-and-stick; chromatin tracing;	M. musculus	LUAD, PDAC	All 20 mouse autosomes	DNA, Proteins	
27 Fujimori, T. et al. Single-cell chromatin state transitions during epigenetic memory formation. <i>bioRxiv</i> (2023).	https://www.biorxiv.org/content/10.1101/20	22	https://data.4dnucleome.org/publications/109b2954-d7d8-43a2-b7a2-83a3fd5da5fc/#expsets-table	ball-and-stick; CT	ORCA	H. sapiens, M. musculus	293T, K562, mouse	human Chr 19; human Chr 8;	DNA	
28 Cheng, Y. et al. Perturb-tracing enables high-content screening of multiscale 3D genome regulators. <i>bioRxiv</i> (2023).	https://doi.org/10.1126/sciadv.adf2245	15	https://data.4dnucleome.org/publications/c4d07d85-7bc4-43d4-bc30-e9b34c1ea8d/#expsets-table	ball-and-stick; CT	ball-and-stick; chromatin tracing	H. sapiens	A549, H1-HEC, RPE-H1TERT	Chromosome 21, 22	DNA	

Legend:

To visualize the FOF-CT compatible datasets associated with this publication, navigate to individual Datasets, Click on Attachments and Click on the "Eye" icon next to the DatasetX.bed file. Example: https://idr.openmicroscopy.org/webclient/omero_table/43412838/

* Jia et al., 2022 (dataset #13) did not generate new datasets but re-analyzed data from Takei et al., 2021 (Nature; dataset #9) and Takei et al., 2021 (Science; dataset #10).

^ Alternative data source: <https://osf.io/ajqyj/>

Table III: Open Microscopy Model compliant Hardware description of the microscopes used to produce published FOF-CT publications and datasets

Nr.	Reference	DOI	Micro-Meta App Microscope 1	Micro-Meta App Microscope 1 Link	Micro-Meta App Microscope 1	Micro-Meta App Microscope 2	Micro-Meta App Microscope 2 Link	Micro-Meta App Microscope 3	Micro-Meta App Microscope 3 Link
1	Wang, S. et al. Spatial organization of chromatin domains and compartments in single chromosomes. <i>Science</i> 353, 598–602 (2016).	https://doi.org/10.1126/science.aaf8084	Harvard-Zhuang_lab_MINA_STORM1_Olympus_ix71-(Wang-2016)	https://data.4dnucleome.org/microscope-configurations/e9aeab9a-8c8f-4e80-b673-20c6c53dc447	Harvard-Zhuang_lab_CT-STORM_Nikon_Eclipse_Ti-U_Bintu-2018_Scope1.json	https://data.4dnucleome.org/microscope-configurations/c8e8a284-c690-4697-9670-822aef7829ef	Harvard-Zhuang_lab_CT-STORM_Nikon_Eclipse_Ti-U_Bintu-2018_Scope2	https://data.4dnucleome.org/microscope-configurations/484f-b8c3-868b6b929e	https://data.4dnucleome.org/microscope-configurations/484f-b8c3-868b6b929e
2	Bintu, B. et al. Super-resolution chromatin tracing reveals domains and cooperative interactions in single cells. <i>Science</i> 362, (2018).	https://doi.org/10.1126/science.aau1783	Harvard-Zhuang_lab_CT-STORM_Nikon_Eclipse_Ti-U_Bintu-2018_Scope1.json	https://data.4dnucleome.org/microscope-configurations/e9aeab9a-8c8f-4e80-b673-20c6c53dc447	Harvard-Zhuang_lab_CT-STORM_Nikon_Eclipse_Ti-U_Bintu-2018_Scope2	https://data.4dnucleome.org/microscope-configurations/484f-b8c3-868b6b929e	Stanford-Boettiger_lab_ORCA_Nikon_Eclipse_Ti-U_Scope2	https://data.4dnucleome.org/microscope-configurations/484f-b8c3-868b6b929e	https://data.4dnucleome.org/microscope-configurations/484f-b8c3-868b6b929e
3	Mateo, L. J. et al. Visualizing DNA folding and RNA in embryos at single-cell resolution. <i>Nature</i> 568, 49–54 (2019).	https://doi.org/10.1038/s41586-019-1035-4	STANFORD-Boettiger_lab_ORCA_Nikon_Eclipse_Ti-U_Scope1.json	https://data.4dnucleome.org/microscope-configurations/84d52890-7e46-4cf8-810c-071ed0673ce8	STANFORD-Boettiger_lab_ORCA_Nikon_Eclipse_Ti-U_Scope2	https://data.4dnucleome.org/microscope-configurations/84d52890-7e46-4cf8-810c-071ed0673ce8	YALE-Wang_Lab_MINA_Nikon_Eclipse_Ti-U_Jellyfish_Config1.json	https://data.4dnucleome.org/microscope-configurations/085f1a9c-1e1a-4a6c-9432-ddf7e6e4e836	https://data.4dnucleome.org/microscope-configurations/085f1a9c-1e1a-4a6c-9432-ddf7e6e4e836
4	Lu, M. et al. Multiplexed imaging of nucleome architectures in single cells of mammalian tissue. <i>Nat. Commun.</i> 11, 2907 (2020).	https://doi.org/10.1038/s41467-020-16732-5	YALE-Wang_Lab_MINA_Nikon_Eclipse_Ti-U_Jellyfish_Config1.json	https://data.4dnucleome.org/microscope-configurations/085f1a9c-1e1a-4a6c-9432-ddf7e6e4e836	YALE-Wang_Lab_MINA_Nikon_Eclipse_Ti-U_Jellyfish_Config1.json	https://data.4dnucleome.org/microscope-configurations/085f1a9c-1e1a-4a6c-9432-ddf7e6e4e836	YALE-Wang_Lab_MINA_Nikon_Eclipse_Ti-U_Jellyfish_Config1.json	https://data.4dnucleome.org/microscope-configurations/085f1a9c-1e1a-4a6c-9432-ddf7e6e4e836	https://data.4dnucleome.org/microscope-configurations/085f1a9c-1e1a-4a6c-9432-ddf7e6e4e836
5	Sawh, A. N. et al. Lamina-dependent stretching and unconventional chromosome compartments in early <i>C. elegans</i> embryos. <i>Mol. Cell</i> 78, 96–111.e6 (2020).	https://doi.org/10.1016/j.molcel.2020.02.006	Harvard-Zhuang_lab_MINA_STORM1_Olympus_ix71-(Wang-2016)	https://data.4dnucleome.org/microscope-configurations/e9aeab9a-8c8f-4e80-b673-20c6c53dc447	UniBase_Biotzentrumbio_Mango_lab_CT_Nikon_Ti2_Scope1	https://data.4dnucleome.org/microscope-configurations/b694ca5d-fc4c-4a7d-b703-dc99adeab5	YALE-Wang_Lab_MINA_Nikon_Eclipse_Ti-U_Jellyfish_Config1.json	https://data.4dnucleome.org/microscope-configurations/085f1a9c-1e1a-4a6c-9432-ddf7e6e4e836	https://data.4dnucleome.org/microscope-configurations/085f1a9c-1e1a-4a6c-9432-ddf7e6e4e836
6	Su, J.-H., Zheng, S. S., Bintu, B. & Zhuang, X. Genome-Scale Imaging of the 3D Organization and Transcriptional Activity of Chromatin. <i>Nature</i> 582, 1641–1659.e6 (2020).	https://doi.org/10.1016/j.cell.2020.07.032	HMS-Zhuang_lab_CT-STORM_Nikon_Eclipse_Ti-U_Su-2020_Scope1.json	https://data.4dnucleome.org/microscope-configurations/0849483d-e203-45e1-b521-1e6e6c8538e0	HMS-Zhuang_lab_CT-STORM_Nikon_Eclipse_Ti-U_Su-2020_Scope2	https://data.4dnucleome.org/microscope-configurations/84d52890-7e46-4cf8-810c-071ed0673ce8	YALE-Wang_Lab_MINA_Nikon_Eclipse_Ti-U_Jellyfish_Config1.json	https://data.4dnucleome.org/microscope-configurations/085f1a9c-1e1a-4a6c-9432-ddf7e6e4e836	https://data.4dnucleome.org/microscope-configurations/085f1a9c-1e1a-4a6c-9432-ddf7e6e4e836
7	Cheng, Y., Liu, M., Hu, M. & Wang, S. TAD-like single-cell domain structures exist on both active and inactive X chromosomes and persist under epigenetic perturbations. <i>Genome Biol.</i> 22, 309 (2021).	https://doi.org/10.1186/s13099-021-02523-8	YALE-Wang_Lab_MINA_Nikon_Eclipse_Ti-U_Jellyfish_Config1.json	https://data.4dnucleome.org/microscope-configurations/085f1a9c-1e1a-4a6c-9432-ddf7e6e4e836	YALE-Wang_Lab_MINA_Nikon_Eclipse_Ti-U_Jellyfish_Config1.json	https://data.4dnucleome.org/microscope-configurations/085f1a9c-1e1a-4a6c-9432-ddf7e6e4e836	YALE-Wang_Lab_MINA_Nikon_Eclipse_Ti-U_Jellyfish_Config1.json	https://data.4dnucleome.org/microscope-configurations/085f1a9c-1e1a-4a6c-9432-ddf7e6e4e836	https://data.4dnucleome.org/microscope-configurations/085f1a9c-1e1a-4a6c-9432-ddf7e6e4e836
8	Huang, H. et al. CTCF mediates dosage- and sequence-context-dependent transcriptional insulation by forming local chromatin domains. <i>Nat. Genet.</i> 53, 1064–1074 (2021).	https://doi.org/10.1038/s41586-021-00863-6	UCSD-Ren_lab_BASCT_Nikon_Eclipse_Ti-U_Lemon.json	https://data.4dnucleome.org/microscope-configurations/84d52890-7e46-4cf8-80b7-aa4691d010e0	YALE-Wang_Lab_MINA_Nikon_Eclipse_Ti-U_Jellyfish_Config1.json	https://data.4dnucleome.org/microscope-configurations/085f1a9c-1e1a-4a6c-9432-ddf7e6e4e836	YALE-Wang_Lab_MINA_Nikon_Eclipse_Ti-U_Jellyfish_Config1.json	https://data.4dnucleome.org/microscope-configurations/085f1a9c-1e1a-4a6c-9432-ddf7e6e4e836	https://data.4dnucleome.org/microscope-configurations/085f1a9c-1e1a-4a6c-9432-ddf7e6e4e836
9	Takai, Y. et al. Integrated spatial genomics reveals global architecture of single nuclei. <i>Nature</i> 590, 344–350 (2021).	https://doi.org/10.1038/s41586-020-03126-2	Caltech-Cai_lab_DNASeqFISH+_Leica_DM8_SpringDisk_Takei_2021_Nature	https://data.4dnucleome.org/microscope-configurations/751988a-ea7a-4140-8507-befa2473f36	YALE-Wang_Lab_MINA_Nikon_Eclipse_Ti-U_Jellyfish_Config1.json	https://data.4dnucleome.org/microscope-configurations/085f1a9c-1e1a-4a6c-9432-ddf7e6e4e836	YALE-Wang_Lab_MINA_Nikon_Eclipse_Ti-U_Jellyfish_Config1.json	https://data.4dnucleome.org/microscope-configurations/085f1a9c-1e1a-4a6c-9432-ddf7e6e4e836	https://data.4dnucleome.org/microscope-configurations/085f1a9c-1e1a-4a6c-9432-ddf7e6e4e836
10	Takai, Y. et al. Single-cell nuclear architecture across cell types in the mouse brain. <i>Science</i> 374, 586–594 (2021).	https://doi.org/10.1126/science.abj1966	Caltech-Cai_lab_DNASeqFISH+_Leica_DM8_SpringDisk_Takei_2021_Nature	https://data.4dnucleome.org/microscope-configurations/751988a-ea7a-4140-8507-befa2473f36	YALE-Wang_Lab_MINA_Nikon_Eclipse_Ti-U_Jellyfish_Config1.json	https://data.4dnucleome.org/microscope-configurations/085f1a9c-1e1a-4a6c-9432-ddf7e6e4e836	YALE-Wang_Lab_MINA_Nikon_Eclipse_Ti-U_Jellyfish_Config1.json	https://data.4dnucleome.org/microscope-configurations/085f1a9c-1e1a-4a6c-9432-ddf7e6e4e836	https://data.4dnucleome.org/microscope-configurations/085f1a9c-1e1a-4a6c-9432-ddf7e6e4e836
11	Limos, G. et al. A leukemia-protective germline variant mediates chromatin module formation via transcription factor nucleation. <i>Nat. Commun.</i> 13, 2042 (2022).	https://doi.org/10.1038/s41467-022-09625-6	STANFORD-Boettiger_lab_ORCA_Nikon_Eclipse_Ti-U_Scope1.json	https://data.4dnucleome.org/microscope-configurations/84d52890-7e46-4cf8-810c-071ed0673ce8	STANFORD-Boettiger_lab_ORCA_Nikon_Eclipse_Ti-U_Scope2	https://data.4dnucleome.org/microscope-configurations/43e1-9ee8-3d6d3174b409	YALE-Wang_Lab_MINA_Nikon_Eclipse_Ti-U_Jellyfish_Config1.json	https://data.4dnucleome.org/microscope-configurations/085f1a9c-1e1a-4a6c-9432-ddf7e6e4e836	https://data.4dnucleome.org/microscope-configurations/085f1a9c-1e1a-4a6c-9432-ddf7e6e4e836
12	Mota, A., Schweißer, M., Wernersson, E., Crosetto, N. & Benko, M. Simultaneous visualization of DNA loci in single cells by combinatorial multi-color IFISH. <i>Sci Data</i> 9, 47 (2022).	https://doi.org/10.1038/s41597-022-01139-2	KarolinskaInstitutet_Benko_lab_CT_Nikon_Eclipse_Ti-U_Scope1.json	https://data.4dnucleome.org/microscope-configurations/71849a75-5a46-41b1-a09-59a4de6628d	YALE-Wang_Lab_MINA_Nikon_Eclipse_Ti-U_Jellyfish_Config1.json	https://data.4dnucleome.org/microscope-configurations/085f1a9c-1e1a-4a6c-9432-ddf7e6e4e836	YALE-Wang_Lab_MINA_Nikon_Eclipse_Ti-U_Jellyfish_Config1.json	https://data.4dnucleome.org/microscope-configurations/085f1a9c-1e1a-4a6c-9432-ddf7e6e4e836	https://data.4dnucleome.org/microscope-configurations/085f1a9c-1e1a-4a6c-9432-ddf7e6e4e836
13	Jia, B. B., Jussila, A., Kern, C., Zhu, Q. & Ren, B. A spatial genome aligner for resolving chromatin architectures from multiplexed DNA FISH. <i>Nat. Biotechnol.</i> 41, 1004–1017 (2023).	https://doi.org/10.1038/s41587-022-01568-9	not applicable	not applicable	YALE-Wang_Lab_MINA_Nikon_Eclipse_Ti-U_Jellyfish_Config1.json	https://data.4dnucleome.org/microscope-configurations/085f1a9c-1e1a-4a6c-9432-ddf7e6e4e836	YALE-Wang_Lab_MINA_Nikon_Eclipse_Ti-U_Jellyfish_Config1.json	https://data.4dnucleome.org/microscope-configurations/085f1a9c-1e1a-4a6c-9432-ddf7e6e4e836	https://data.4dnucleome.org/microscope-configurations/085f1a9c-1e1a-4a6c-9432-ddf7e6e4e836
14	Murphy, S. E. & Boettiger, A. N. Polycopy repression of Hox genes involves spatial feedback but not domain compaction or phase transition. <i>Nat. Genet.</i> 53, 493–504 (2024).	https://doi.org/10.1038/s41586-024-06616-1	STANFORD-Boettiger_lab_ORCA_Nikon_Eclipse_Ti-U_Scope2	https://data.4dnucleome.org/microscope-configurations/085f1a9c-1e1a-4a6c-9432-ddf7e6e4e836	STANFORD-Boettiger_lab_ORCA_Nikon_Eclipse_Ti-U_Scope3	https://data.4dnucleome.org/microscope-configurations/43e1-9ee8-3d6d3174b409	YALE-Wang_Lab_MINA_Nikon_Eclipse_Ti-U_Jellyfish_Config1.json	https://data.4dnucleome.org/microscope-configurations/085f1a9c-1e1a-4a6c-9432-ddf7e6e4e836	https://data.4dnucleome.org/microscope-configurations/085f1a9c-1e1a-4a6c-9432-ddf7e6e4e836
15	Hafner, A. et al. Loop stacking organizes genome folding from TADs to chromosomes. <i>Mol. Cell</i> 83, 1377–1392.e6 (2023).	https://doi.org/10.1016/j.molcel.2023.04.008	STANFORD-Boettiger_lab_ORCA_Nikon_Eclipse_Ti-U_Scope2	https://data.4dnucleome.org/microscope-configurations/085f1a9c-1e1a-4a6c-9432-ddf7e6e4e836	STANFORD-Boettiger_lab_ORCA_Nikon_Eclipse_Ti-U_Scope3	https://data.4dnucleome.org/microscope-configurations/085f1a9c-1e1a-4a6c-9432-ddf7e6e4e836	YALE-Wang_Lab_MINA_Nikon_Eclipse_Ti-U_Jellyfish_Config1.json	https://data.4dnucleome.org/microscope-configurations/085f1a9c-1e1a-4a6c-9432-ddf7e6e4e836	https://data.4dnucleome.org/microscope-configurations/085f1a9c-1e1a-4a6c-9432-ddf7e6e4e836
16	Chen, L.-F. et al. Structural elements promote architectural stripe formation and facilitate ultra-long-range gene regulation at a human disease locus. <i>Nat. Genet.</i> 55, 306–314 (2023).	https://doi.org/10.1186/s13098-023-01641-2	STANFORD-Boettiger_lab_ORCA_Nikon_Eclipse_Ti-U_Scope1	https://data.4dnucleome.org/microscope-configurations/84d52890-7e46-4cf8-810c-071ed0673ce8	STANFORD-Boettiger_lab_ORCA_Nikon_Eclipse_Ti-U_Scope2	https://data.4dnucleome.org/microscope-configurations/43e1-9ee8-3d6d3174b409	YALE-Wang_Lab_MINA_Nikon_Eclipse_Ti-U_Jellyfish_Config1.json	https://data.4dnucleome.org/microscope-configurations/085f1a9c-1e1a-4a6c-9432-ddf7e6e4e836	https://data.4dnucleome.org/microscope-configurations/085f1a9c-1e1a-4a6c-9432-ddf7e6e4e836
17	Hung, T.-C., Kingsley, D. M. & Boettiger, A. N. Boundary stacking interactions enable cross-TAD enhancer-promoter communication during limb development. <i>Nat. Genet.</i> 56, 306–314 (2024).	https://doi.org/10.1186/s13098-023-01641-2	STANFORD-Boettiger_lab_ORCA_Nikon_Eclipse_Ti-U_Scope1	https://data.4dnucleome.org/microscope-configurations/085f1a9c-1e1a-4a6c-9432-ddf7e6e4e836	STANFORD-Boettiger_lab_ORCA_Nikon_Eclipse_Ti-U_Scope2	https://data.4dnucleome.org/microscope-configurations/43e1-9ee8-3d6d3174b409	YALE-Wang_Lab_MINA_Nikon_Eclipse_Ti-U_Jellyfish_Config1.json	https://data.4dnucleome.org/microscope-configurations/085f1a9c-1e1a-4a6c-9432-ddf7e6e4e836	https://data.4dnucleome.org/microscope-configurations/085f1a9c-1e1a-4a6c-9432-ddf7e6e4e836
18	Patterson, B. et al. Female naïve pluripotent stem cells carry X chromosomes with X-like and X-like folding conformations. <i>Sci. Adv.</i> 9, eabf2245 (2023).	https://doi.org/10.1126/sciadv.adf2245	YALE-Wang_Lab_MINA_Nikon_Eclipse_Ti-U_Jellyfish_Config1.json	<a href="https://data.4dnucleome.org/microscope-configurations/085f1a9c					